U.S. Department of the Interior
U. S. Geological Survey
Open–File Report 96–523

Coactive Fault of the Northridge Earthquake—Granada Hills Area, California

(Evidence that coactive faulting could have caused much of the damage in the Granada Hills area during the 17 January 1994, Northridge, California earthquake)

by

Arvid M. Johnson
Robert W. Fleming
Kenneth M. Cruikshank
and
Robert F. Packard

Denver, Colorado
1996

Coactive Fault of the Northridge Earthquake—Granada Hills Area, California

Arvid M. Johnson
Department of Earth and Atmospheric Sciences
Purdue University
West Lafayette, Indiana 47907
(317) 494–0250 (Fax: 496–1210)

Robert W. Fleming
Geologic Hazards Team
U.S. Geological Survey, Mail Stop 966
Denver, Colorado 80225
(303) 273–8603 (Fax: 8600)

Kenneth M. Cruikshank
Department of Geology
Portland State University
Box 751
Portland, Oregon 97207
(503) 725–3383 (Fax: 3025)

Robert F. Packard
Survey Division
Bureau of Engineering
Department of Public Works
16th floor, 600 S. Spring
Los Angeles, California 90014

Abstract

The most important result of this research supports a growing body of evidence that any active fault that approaches the ground surface, or cuts the surface in an area, has the potential of moving coactively in a major earthquake sequence in that area. Coactive movement produces high, localized ground deformation and, therefore, extensive localized damage to structures, utilities, highways, and other lifelines. Observations and measurements have demonstrated that intense ground deformation during an earthquake sequence is not restricted to a band a few meters wide, or even a belt a few hundreds of meters wide along the trace of a fault that produces an earthquake sequence.

This is a study of localized ground deformation along structural features that activated during the 1994 Northridge earthquake sequence in the Granada Hills area. Because the Northridge earthquake sequence occurred in a highly–developed metropolitan area, survey and deformation data are available that do not exist in more rural settings. In this paper, we present results of survey leveling and angular and length changes between benchmarks that were obtained by the City of Los Angeles. These data are compared to an extensive record of ground deformation in the same area, compiled and presented by Hecker and others (1995a). Inferences from the survey data and kinematic interpretation of the deformational data are shown, by model, to indicate a hidden or buried structure as the cause for the pattern. Individually and collectively, these data for the Granada Hills area of the San Fernando Valley point to a deep–seated disturbance, such as a reverse fault or shear zone. The principal elements of the results leading to this conclusion are as follows: (1) There is a local steepening of contours of vertical uplift and adjacent depression of contours on the hanging–wall block that moved during the main shock of the Northridge earthquake sequence. (2) There is a belt of extension fractures in the northern part of the Granada Hills area and a subparallel belt of compression structures in the southern part of the area. (3) Measurements of length and angle changes among subsurface monuments at street intersections produce extension figures which form belts that closely track the belts of extensile and compressive ground damage in the area. (4) A theoretical model of relaxation of resistance to slip on a simple reverse fault, dipping northward beneath a free surface, qualitatively reproduces the local concentration of differential vertical uplift and adjacent depression together with associated belts of high extension and compression.

Acknowledgments

This research would not have been possible without the generous and enthusiastic efforts of the Survey Division, City of Los Angeles. In particular, we wish to thank William Prange, Surveyor, Robert Jones, Surveyor, Robert Renison, Supervisor of Surveying and Robert Taylor, Acting Engineer of Surveys. All these people have been extremely helpful as we worked with their data.

This paper is part of a broader study, a collaboration of the City of Los Angeles Department of Surveys, the U.S. Geological Survey, and Purdue University through grants from the Nuclear Regulatory

Commission (Fleming), The Federal Emergency Management Agency (Packard), the National Science Foundation EAR 9416760 (Johnson and Cruikshank) the Department of Energy DE FG02 93ER14365 (Johnson) and the Southern California Earthquake Center NTP2898 (Johnson). We appreciate the support of these organizations. Nils A. Johnson drafted the maps and figures. Edward Cranswick, U.S. Geological Survey, reviewed the manuscript. Jim Gardner, technical editor in Earth and Atmospheric Sciences, edited the manuscript. We thank these people for improving the manuscript, but we are responsible for remaining errors.

Introduction

Coactive Faults

The 1994, Northridge, California earthquake illustrates that a large earthquake sequence includes rupture along both a main fault and nearby faults with quite different kinematic signatures. In previous papers we have shown that, where the main fault reaches the ground surface, there are broad zones of damage—50 to 200 m wide at Landers, California, for instance—that can be recognized by studying and mapping kinematic details of the ground fracturing (Johnson and Fleming, 1993; Johnson and others, 1993, 1994). This ground deformation can be largely responsible for the damage to man–made structures (e.g., Lazarte and others, 1994). There is another problem, though, which we emphasized in the discussion of our paper on left–lateral fractures at Loma Prieta (Johnson and Fleming, 1993). Our concern was, and continues to be, that by relegating fault slip to fault surfaces deep beneath an epicentral area, we may be overlooking evidence of coseismic slip along ground ruptures in an epicentral area, as was done at Loma Prieta, and we may also fail to recognize the significance of nearby coactive faulting and shearing (Holzer, 1994). The ground deformation caused by slippage on coactive faults and shear zones in the area of the fault that produced the main shock of an earthquake sequence may be responsible for much of the damage to streets, highways, office buildings and dwellings. If, in fact, further research supports the notion of coactive faults during earthquakes, then predictions of earthquake damage must change focus from the main faults and the ground shaking attendant to the main fault, to include faults that might move coactively with the main fault. These may be faults that generate aftershocks, or faults or shear zones that move aseismically. In either case, we recognize that damage to man–made structures may be caused by ground deformation accompanying slip on coactive faults, rather than by ground shaking.

The evidence for significant ground deformation along coactive faults is particularly strong at Northridge. The fault that produced the main shock should reach the ground surface to the north, in the Santa Susana Mountains, whereas there are fault–like belts of surface damage within the San Fernando Valley. Evidence for coactive faulting, however, was recognized at least as early as the time of the Borrego Mountain earthquake sequence. Several strike–slip faults in southern California were coactive with the 1968, Borrego Mountain earthquake sequence on the Coyote Creek Fault (Allen and others, 1972), even though they were far outside the area of aftershock activity. Allen and others described evidence for coactive slip on the

Imperial, Superstition Hills, and San Andreas fault zones. Another clear example of coactive faulting during a large earthquake sequence was documented at Loma Prieta by Haegerud and Ellen (1990) for range–front thrust faults, Aydin and others (1992) for the Sargent fault, and Johnson and Fleming (1993) for the Summit Ridge shear zone in the epicentral area. The range–front faults extended 30 to 40 km, from Los Gatos in the SE to Los Altos Hills and Stanford in the NW (Plafker and Galloway, 1989; Haegerud and Ellen, 1990).

For the Borrego Mountain earthquake sequence the coactive slip on nearby faults was right lateral, which is the same as the right lateral on the fault responsible for the main shock. For the Loma Prieta earthquake sequence, the coactive slip on nearby faults was right lateral in some areas but SW side up reverse faults along the range front faults whereas the slip on the fault responsible for the main shock was SW side up reverse/right–lateral.

Northridge Earthquake Sequence

The Northridge earthquake event was a sequence of hundreds, or thousands, of earthquakes, many of which were not on the fault that produced the main shock (Hauksson and others, 1995). The main shock of the Northridge earthquake (6.7 Ms), was at 12:31 UTC (4:31 a.m., Pacific Time), 17 January 1994. The hypocenter was about 14 km beneath the town of Northridge in the San Fernando Valley, and significant damage was caused up to 64 km from the epicenter (Figure 1). The sense of differential displacement on the main fault was predominantly reverse, with the southern block upthrown. The main fault attributed to the earthquake strikes N70° –80°W and dips 35°–45° south (Hauksson and Jones, 1994). Had it propagated with this orientation to the ground surface, the fault rupture would have appeared in the vicinity of the crest of the Santa Susana Mountains to the north of the San Fernando Valley.

Our investigation is generally in the San Fernando Valley, and the specific study reported here centers on the Granada Hills area, about 6 km north of Northridge, in the hanging–wall block of the main fault.

Tectonic Setting

The general tectonic setting of the Northridge earthquake sequence is well known. The Los Angeles area is immediately south of the Transverse Ranges, where the broad band of generally right–lateral San Andreas fault systems south of Los Angeles take a left jog and reorganize into a narrower band of strike–slip faults north of the Transverse Ranges, producing an area of roughly north–south compression within the Transverse Ranges. Northridge is essentially the bullseye of the area of compression within the Transverse Ranges. It is in the San Fernando Valley, a broad, roughly east–west trending basin between the Santa Susana Mountains to the north and the Santa Monica Mountains to the south (Figure 1).

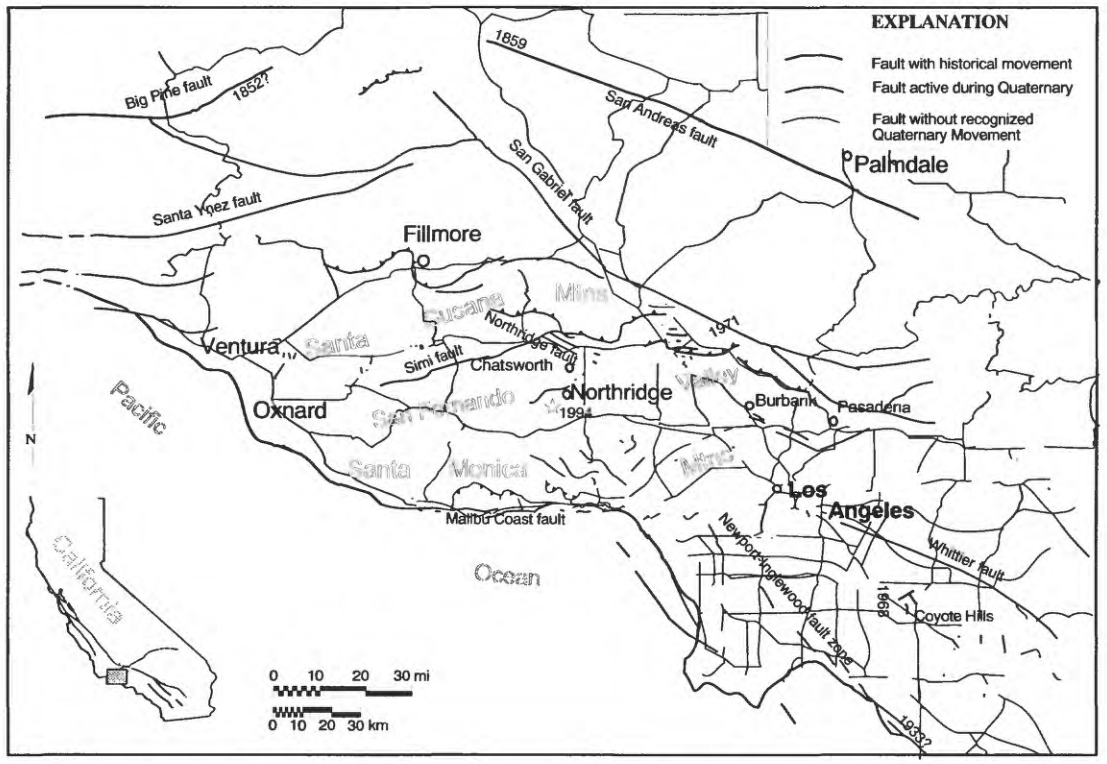

Figure 1. Location of the Northridge earthquake, showing locations of various faults that have been recognized in the area. Time of latest movement during an earthquake is indicated by a year.

San Fernando Valley Heart Structure

More nearly locally, the tectonic setting of the Northridge earthquake sequence is within the San Fernando Valley heart structure[1] (Figure 2; after Wei and Johnson, in prep.). In its simplest form, a heart structure is a faulted fold produced where a dish fault is subjected to horizontal compression, which causes an anticline to form over the two tips of the fault (Figure 3) and a syncline to form in-between. The cross–section shown in Figure 2 is a smoothed version of a cross–section of the San Fernando Valley area presented by Davis and Namson (1994), based on an interpretation of data that includes shallow wells (up to about 2 or 3 km depth), surface geology, unspecified deep drilling, and, presumably, seismic profiles. The San Fernando Valley heart structure, which is some 35 km wide and 20 km deep, is similar in many ways to the theoretical form (Figure 3). The dish fault within the heart structure is defined on the northeast by the Pico thrust and on the southwest by the Santa Monica thrust (Figure 2). According to this tectonic interpretation, then, the Santa Monica Mountains would be the narrow anticline on the southwestern side of the heart structure and the Santa Susana Mountains would be the narrow anticline on the northwestern side. These "narrow" folds are some 10 km wide. Between is the broad syncline, represented by the San Fernando Valley itself. The structures beneath the San Fernando structure are too poorly known to relate to a theoretical model.

[1]Also known as a "pop-up structure" and a "delta structure."

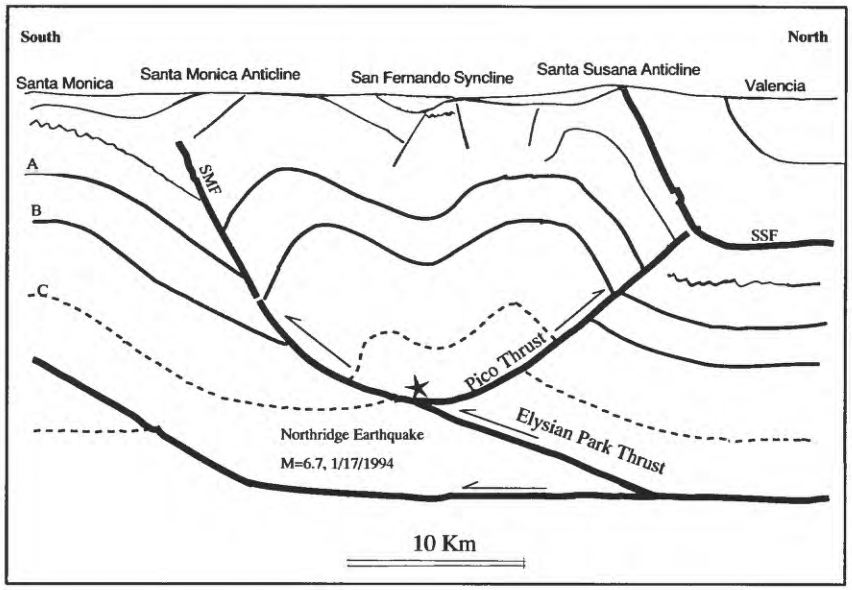

Figure 2. Interpretative structural cross–section of San Fernando Valley area, showing a dish–shaped fault that underlies the center of the valley and that ends beneath the Santa Monica Mountains to the south and the Santa Susana Mountains to the north. (Map modified after Davis and Namson, 1994). The epicenter of the Northridge earthquake was at about 19 km depth, apparently along the Pico thrust fault. The Pico thrust fault is interpreted to be listric in order to explain the tilting of the San Fernando Valley toward the south. SSF = Santa Susana fault, SMF = Santa Monica fault)

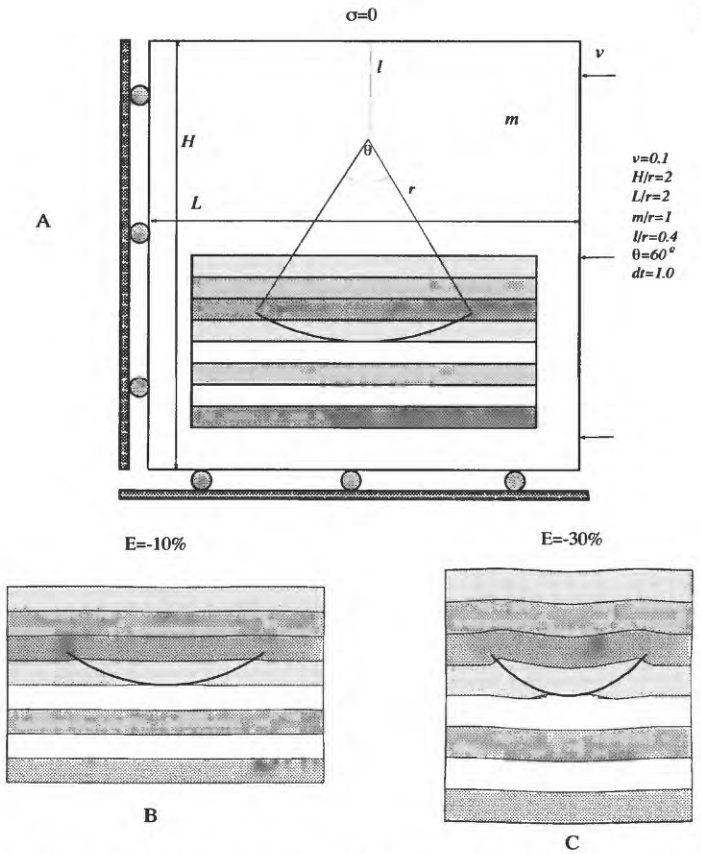

Figure 3. Heart structure, a type of faulted fold (after Wei and Johnson, in prep.). The heart structure is produced by a dish fault in homogeneous flowing material with passive markers. The flowing material is incompressible, so the cross–section is balanced. A. Loading conditions, consisting of uniform shortening and thickening. B. Form of passive layering after 10% shortening. Heart structure is starting to take form. C. Form of passive layering, defining a clear heart structure, after 30% shortening.

The epicenter of the main shock of the 1994 Northridge earthquake was at a depth of about 18 km, apparently on the Pico thrust. The slip near the epicenter was about 2.5 m, with the hanging wall pushed upward.

Possible Explanation for Tilting of Valley

The most obvious feature of the uplift pattern in the San Fernando Valley is the relatively–uniform tilting of the floor of the valley from southwest to northeast. Davis and Namson constructed the San Fernando Valley structure as their typical stick figure[1], with planar faults (1994), but in order to explain the tilting we have reconstructed it with cylindrical, listric faults (Figure 2). The planar fault shown by Davis and Namson cannot explain the pattern of changes in ground altitude in the San Fernando Valley and the Santa Susana Mountains. The tilting pattern is shown in Plate 1, a map of contours of differential uplift in the San Fernando Valley between 1980 and 1994[2]. The area of uplift was evidently more extensive than the area shown here (Hudnut and others, 1996). The pattern in the San Fernando Valley is fan–shaped—that is, like that of an alluvial fan—with a maximum uplift value of about 0.5 m in the Santa Susana Mountains in the north, but a few km south of the area where one might project the fault that produced the main shock to the ground surface.

We suggest that the uniform tilting is a result of slippage primarily on the Pico thrust, the fault that produced the main shock. If the Pico thrust is listric[3], as shown in Figure 2, then slippage would cause the observed tilting of the hanging–wall block (Wei and Johnson, in prep.).

On the basis of the slip, δs=2.2 m, on the Pico fault (Shen and others, 1996), and the regional gradient, $\delta\theta$, of vertical displacement, we can estimate the average radius of curvature of the part of the Pico thrust fault that slipped during the earthquake sequence. According to Plate 1, the average gradient in vertical uplift across the San Fernando Valley is $\delta\theta=3.1\times10^{-5}$. We obtain an estimate of the regional gradient of $\delta\theta=3.5\times10^{-5}$ for the Granada Hills area. Based on these values, and the equation,

$$\delta s=\rho\ \delta\theta$$

we determine that, for the first estimate of gradient, the average radius of the part of the Pico thrust that slipped was ρ= 63 to 71 km. So we estimate a radius of curvature of 67 km for the part of the Pico thrust fault that slipped during the earthquake sequence. These values seem reasonable on the northern limb of the dish fault (Figure 2), away from the trough. In the trough, the radius of curvature is about 11 km.

---

[1]See comments by Stone, 1996; Johnson and Fletcher, 1994, p. 5–7, 387.

[2]The City of Los Angeles ran level lines along several streets in the San Fernando Valley after the Northridge earthquake, including north–south streets Resida Boulevard, Topanga Canyon Boulevard, Van Nuys Boulevard, and part of Balboa Boulevard, and east–west streets Devonshire Street, Roscoe Boulevard, Ventura Boulevard and part of Rinaldi Street. The level lines had been run previously in 1980, so the results show changes in altitude between 1980 and 1994. The reference point, assumed not to have moved vertically, was selected to be in Woodland Hills, along Topanga Canyon Boulevard, about 2 km south of Highway 101. Please see acknowledgements for the surveyors who provided the information reported here.

[3]Others probably have recognized evidence for a listric form of the fault that produced the main shock at Northridge. Hauksson and others (1995, p. 12,339) refer to a possible listric shape as follows: A..."difference in the main shock focal mechanism determined with different frequency waves suggests a small increase in dip along strike and possibly a curved rupture surface."

The most troubling feature of the relatively–uniform tilting of the San Fernando Valley floor, from southwest to northeast is that, if continued, the pattern would not produce the San Fernando Valley basin. It is perhaps important to realize, though, that a single earthquake sequence may be only a stage in the growth of a tectonic structure. Perhaps the Northridge earthquake sequence along the Pico thrust, and related faults to the northeast, represents growth of only the northern part of the San Fernando Valley heart structure. Growth of the southern part may be waiting for an earthquake sequence on the Santa Monica fault zone that underlies the southern half of the heart structure (Figure 2).

Perturbations in Vertical Displacement

If movement on the Pico fault and tilting of the San Fernando Valley during the Northridge earthquake sequence are first–order tectonic phenomena, then second–order phenomena, perhaps associated with smaller faults, appear to be represented by several interruptions of the smooth, tilted fan shape in four areas. These are at Sherman Oaks/Van Nuys, Northridge/Winnetka, Chatsworth, and Granada Hills (Plate 1). In the area between Sherman Oaks and Van Nuys, at the foot of the Santa Monica Mountains, there is a broad (about 3 or 4 km wide) region, north–south, within which the relative change in altitude is nearly zero (Plate 1). It is expressed as a flattening of the surface of differential vertical uplift and may well be associated with an increase in uplift to the south. This kinematic picture is consistent with the position of the feature at the foot of uplifted mountains. Another area of flattening of the surface of differential vertical uplift is in the vicinity of Winnetka, Northridge and Cal State Northridge (Plate 1). This area is expressed as a bowing outward of contours to the north and south around a weak high near the intersection of Saticoy Street and Resida Boulevard. Again, the shape of this feature could be explained in terms of slip on a fault or shear zone, trending northeastward. There is a fault without recognized Quaternary movement following this trend on the preliminary fault map of California (Figure 1) (Jennings, 1973).

The two areas where the gradient in differential vertical uplift appears to be highest are along the southern foothills of the Santa Susana Mountains. One consists of a very steep gradient across Devonshire Street in Chatsworth (Plate 1), and a distinctive low south of the street. This feature could represent, kinematically, a reverse fault or shear zone dipping northward beneath the Santa Susana Mountains. Its location is coincident with the Northridge fault (Figure 1), a fault with evidence of Quaternary movement (Jennings, 1973). The kinematics are consistent with the uplift of the Santa Susana Mountains along a reverse fault or downdropping of the San Fernando Valley along a normal fault. The second area of perturbation of the general fan shape, with a steep gradient to the northwest and a deep depression to the southeast, is in the area of the study reported here, in Granda Hills, between Rinaldi and Lorillard streets (Plate 1).

In this paper we affirm the conclusion of Hecker and others (1995b), that there was significant permanent ground deformation in the Granada Hills area during the 1994 Northridge, California, earthquake sequence, and that the strains representing this deformation can be correlated with much of the damage to structures, and with types and distributions of ground fractures mapped by Hecker and others (1995a). This pattern of ground deformation is consistent with defor-

mation produced by a reverse fault or shear zone segment dipping north, beneath the Santa Susana Mountains, or a normal fault segment dipping south, beneath the San Fernando Valley.

Method of Study of Deformation in Granada Hills Area

Our study involves field work—examining fractures in sidewalks, streets and houses—in the Balboa area, for 1 week shortly after the January 1994 earthquake sequence, and for 5 days during the spring and summer of 1995. Although we made notes and some measurements, we did not make detailed maps. Members of the U.S. Geological Survey, however, mapped damage to houses and ground fractures in the Granada Hills and Mission Hills areas immediately after the earthquake sequence, providing detailed information to compare to our study.

Most of our study involves analysis of measurements of horizontal positions of monuments made by surveyors of the City of Los Angles in 1972, 1983, and 1994. The surveys are compared to those made by private contractors at the time the Rinaldi Street/Balboa Boulevard area of Granada Hills was developed in the 1960's.

The Granada Hills Area

Saul (1974) described the geology of the Granda Hills area as part of his study of the San Fernando earthquake of 1971. He presents stratigraphic evidence for very recent faulting and growth of folds in Late Tertiary and Quaternary sedimentary rocks in the area. He recognized the Mission Hills anticline trending east–west near the Lower San Fernando Dam, in the east part of the area (Figure 4), and the Hadley anticline trending northwest immediately north of the Northridge fault (Figure 1), (Saul, 1974, fig. 1). He also recognized several faults and fault zones, including the Northridge Hills fault zone north of Chatsworth (Figure 1), the Devonshire fault zone within the Hadley anticline, and the Mission Hills fault, a U–shaped fault that cuts through the center of the Granada Hills area of our study (Figure 4). A few other faults in the area (Figure 4) are shown in maps by Oakeshott (1958), Barnhart and Slosson (1973), and Barrows and others (1974).

With the same data on relative altitude change used to construct the contours of altitude change shown in Plate 1, we have reinterpreted it to conform with the eastern part of the Mission Hills fault (Figure 4). Thus interpreted, the map suggests growth of a plunging syncline centered on Index Street and plunging anticlines in Granada Hills near Devonshire Street and the Lower San Fernando Dam. The interpretation in Plate 1 shows essentially the same anticlines, but the syncline is replaced with a basin. Both interpretations, of course, are arbitrary.

The Surveys

Repeated surveys of streets throughout the Los Angeles area provide unusually detailed information about horizontal components of ground deformation during earthquakes. Throughout the city, the relative horizontal positions of monuments at most street intersections and, in places, even between street intersections, have been measured on a periodic basis. The first surveys were made by contractors in most areas. But after the 1971 San Fernando earthquake sequence, many intersections throughout the entire city were resurveyed. In our study area in Granada Hills, the resurvey had been done in 1972. Resurvey of part of our study area

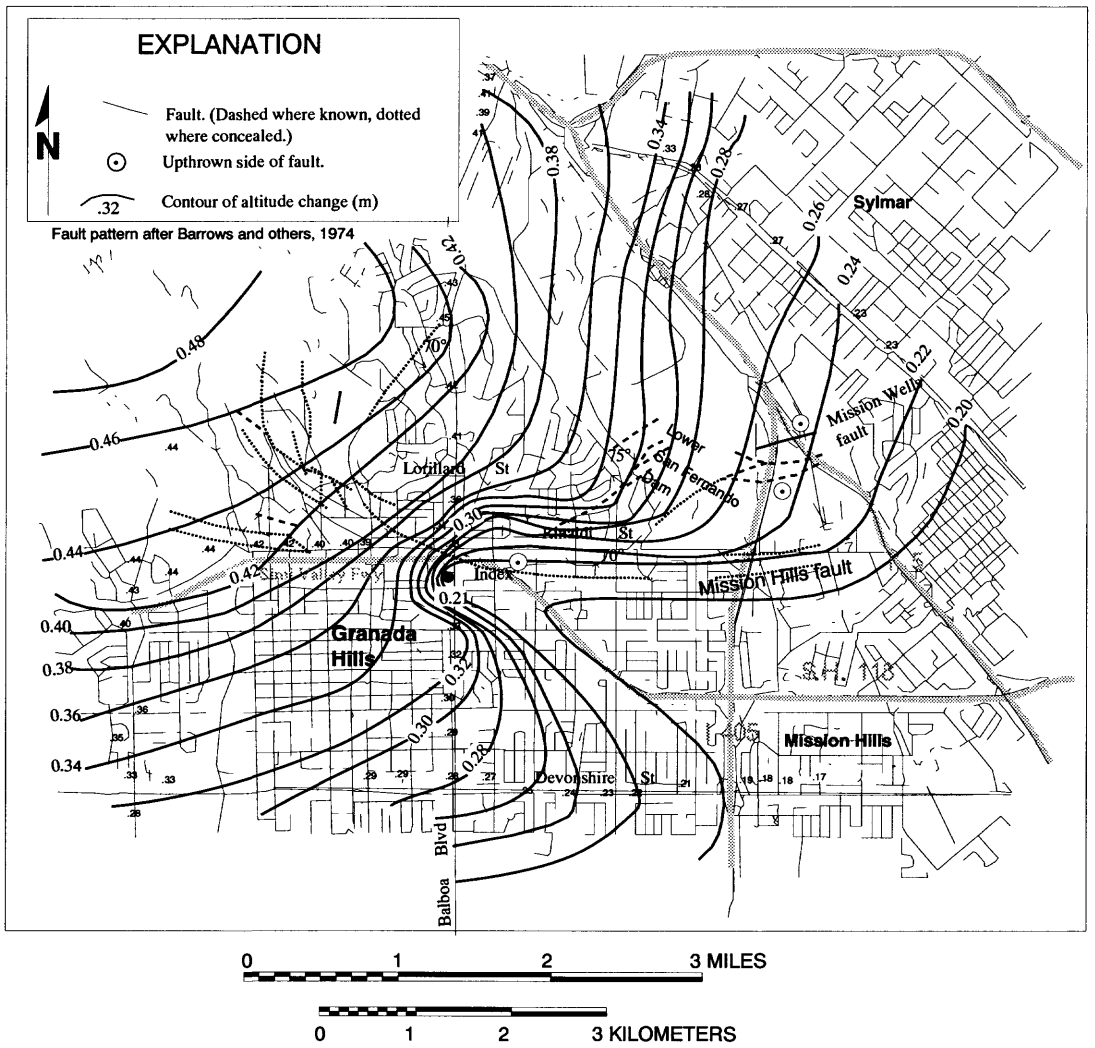

Figure 4. Faults in Granada Hills area (after Barrows and others, 1974 and Saul, 1974) and contour map of changes in altitude during the 1994 Northridge earthquake. The deep plunging syncline centered on Index Street is intended to relate to the Mission Hills fault. The area of our detailed study is between Rinaldi and Lorillard, on either side of Balboa Boulevard.

had been done in 1983, and the entire area was resurveyed in 1994 and 1995, following the Northridge earthquake sequence of 1994.

Details of the surveying techniques and accuracy of measurements are discussed in Appendix I. As indicated there, the survey points are center–line monuments for the City of Los Angeles, (Robert Jones, pers. comm., 1995), located at the centerlines of roads and at the center of intersections. These include surface and subsurface monuments. Subsurface monuments are of two types, both of which are anchored to ground beneath the road–fill prism. One is a special target hole punched into a cap on a steel pipe, encased in concrete below road level (generally the top of the target is about 0.3 m below the road surface). These targets are accessed through steel covers, about 10 cm in diameter, at road level. The second is a series of four punch marks in the sides of sewer access vaults. The access vaults extend below the road–fill material to the sewer level. The punches are at a depth of about 0.5 m. The point where lines

connecting opposing punches cross is the target in these cases.

Surface monuments are normally spikes or nails driven into the pavement through a washer or a circle of tin, but they may be a lead–filled hole with a small tack driven into the lead or a railroad spike with a punched hole.

Both subsurface and surface center–line monuments are generally backed up by four points known as "tie outs," which are monuments a known distance and direction from the center–line monuments. Generally tie–outs are used to determine the area for a careful search for a center–line monument, but they can also be used to re–establish destroyed center–line monuments.

According to city surveyor Robert Jones (1995, pers. comm.), the City of Los Angeles regards their determination of distances to be accurate to 3.1 mm. For a street length of 100 m, the normalized error would be 3×10^{-5}. In interpreting the strain patterns from this study we have assumed that normalized length changes must be at least three times this great, at least 10^{-4}, to be significant. Angle measurements should have an error of less than 3 seconds. The corresponding error in shear strain is the tangent of the angle, so the error is 1.45×10^{-5}. Thus angle measurements have an error that is less than distance measurements, and shear strains can again be determined to about 10^{-5}. We use 10^{-4} as a cutoff for strain determinations, so strains judged to be significant are about an order of magnitude larger than the instrument error.

There are, of course, other sources of error. For example, in the Balboa area some of the center–line intersection monuments were relocated using tie–outs, or from matching centerlines of adjacent streets. The error of location for these monuments is expected to be as large as 3 cm, so the length measurements from these intersections would be in doubt by that amount (Intersections 17, 19, 20, 26, 29, and 50, Appendix II). In fact, the changes due to deformation are generally much greater than this, so that the magnitudes of the strains, but not the senses of shortening or lengthening, will be changed for those intersections.

We note that along Balboa Boulevard, the total change in length between center–line monuments is the same as the change in length determined using the survey of lot marks along the sidewalk.

Other details are presented in Appendix 1.

Calculation of Extensions and Strains

We can use the resurveys to calculate the strains for each corner of an intersection, provided that we can reasonably assume that, at the scale of the street lengths, the strains are homogeneous. The method is invalidated where there are large fractures that accommodated most of the changes in positions of the adjacent monuments. In the theoretical discussion presented here, we assume that such fractures are absent.

General Problem. Consider two intersecting street segments, 0a and 0b (Figure 5). We select a to be the length of the street trending roughly east–west. Actually, the a street is oriented at an easterly angle, α. The intersecting street is then b (Figure 5B). We use upper–case letters for the reference (initial) state and lower–case for the current (final) state in computing strains. For the final state, the b–street is at some angle θ from the a–street, measured in a counterclockwise sense (Figure 5B), and for the initial state, the B–street is at some angle Θ from the A–street (Figure 5A). The streets are not necessarily at right angles. These are the coordinates and lengths we select to describe the deformations.

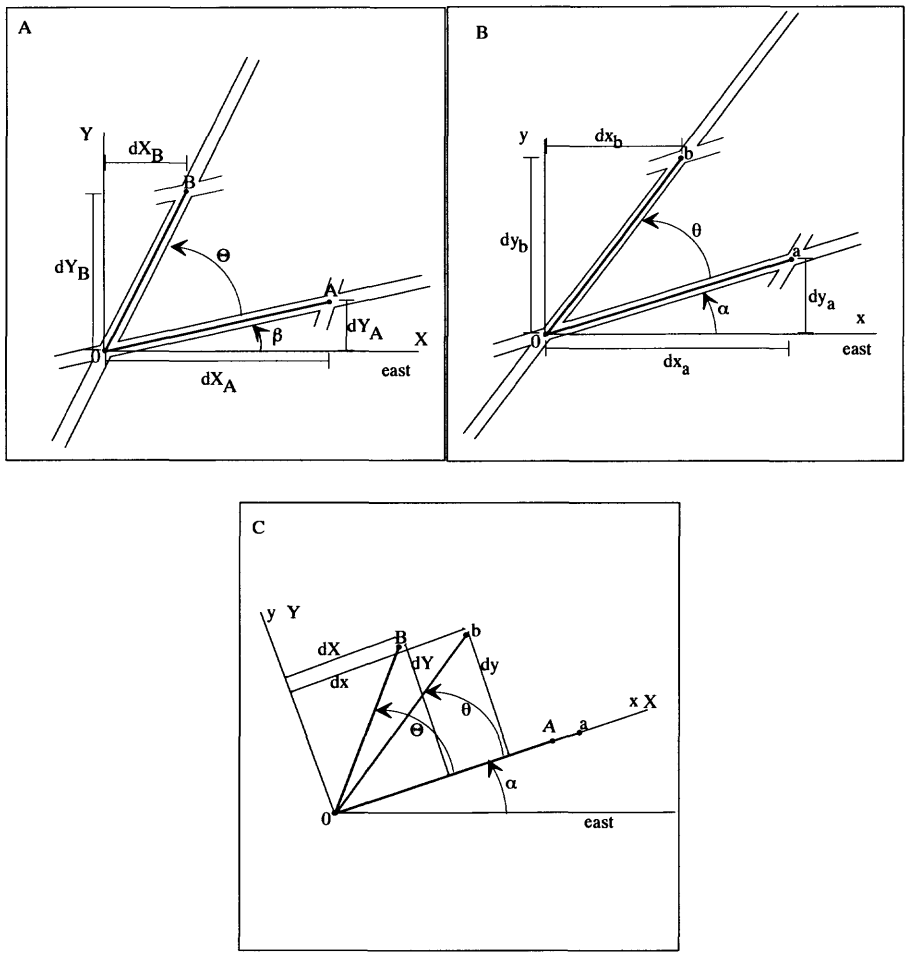

Figure 5. Lengths and angles of street segments used to compute deformations at intersections in the Granada Hills area. A. Hypothetical original street pattern, surveyed prior to the 1994 earthquake (in the 1960's, or 1972, or 1983). The initial state is represented by capital letters. B. Deformed intersection, after the 1994 earthquake, showing new lengths and angles. The deformed state is represented by lower–case letters. C. Special case assumed for computations because information is lacking on compass orientations of streets. Lengths such as 0A and 0a, 0B and 0b, and angles Θ and θ are known, but angles α and β are unknown. For the calculations, street segments 0A and 0a are assumed to be parallel before and after the earthquake sequence, and the x– and X–axes are chosen to be parallel to these segments. Only the rotational part of the deformation is missed by this special assumption.

The method that we use to calculate strains in the Balboa area is a special case of strain theory, (e.g., Johnson and Pollard, in prep.; Malvern, 1976). In this case, we use measurements and strain theory to compute the components of the deformation tensor, F_{iJ},

$$F_{iJ} = (\partial x_i / \partial X_J) \qquad (1)$$

which generally has nine independent components for three–dimensional deformations, and where $x_1 = x$, $x_2 = y$, $x_3 = z$, $X_1 = X$ and so forth. The components of strains are related to the components of deformation gradient through the relation,

$$\varepsilon_{IJ} = (1/2)[(\partial x_k / \partial X_I)\,(\partial x_k / \partial X_J) - \delta_{IJ}] \qquad (2)$$

which has principal strain values, ε_1 and ε_2.

The complete state of strain is expressed in terms of the components of the deformation

gradient, as indicated in eq. (2). The available survey data lacks information about changes in the vertical, z, direction, so we can determine only four independent components, $(\partial x/\partial X)$, $(\partial x/\partial Y)$, $(\partial y/\partial Y)$, and $(\partial y/\partial X)$. In order to compute the four components of the deformation gradient from complete survey data, we can proceed as follows. Consider Figures 5A and 5B, which show a street intersection before (Figure 5A) and after (Figure 5B), a deformation. We have two line elements, street segment A and street segment B, before and after the deformation. dX_A is the projection of line element A onto the X–axis and dY_A is the projection of line element A onto the Y–axis. Thus, for line element A before and a after the deformation, we can write the relations involving the components of the deformation gradient

$$dx_a = (\partial x/\partial X)dX_A + (\partial x/\partial Y)dY_A \qquad (3a)$$

$$dy_a = (\partial y/\partial X)dX_A + (\partial y/\partial Y)dY_A \qquad (3b)$$

or, in terms of the known lengths and angles shown in Figure 5A and 5B,

$$a\cos(\alpha) = (\partial x/\partial X)\,A\cos(\beta) + (\partial x/\partial Y)\,A\sin(\beta)$$

$$a\sin(\alpha) = (\partial y/\partial X)\,A\cos(\beta) + (\partial y/\partial Y)\,A\sin(\beta)$$

or,

$$S_a\cos(\alpha) = (\partial x/\partial X)\cos(\beta) + (\partial x/\partial Y)\sin(\beta) \qquad (4a)$$

$$S_a\sin(\alpha) = (\partial y/\partial X)\cos(\beta) + (\partial y/\partial Y)\sin(\beta) \qquad (4b)$$

in which the stretch, S_a, is

$$S_a = a/A \qquad (4c)$$

Similarly, considering the line element B, we derive,

$$S_b\cos(\theta+\alpha) = (\partial x/\partial X)\cos(\Theta+\beta) + (\partial x/\partial Y)\sin(\Theta+\beta) \qquad (4d)$$

$$S_b\sin(\theta+\alpha) = (\partial y/\partial X)\cos(\Theta+\beta) + (\partial y/\partial Y)\sin(\Theta+\beta) \qquad (4e)$$

in which the stretch, S_b, is

$$S_b = b/B \qquad (4f)$$

Thus, if we can measure the stretches of the two streets, S_a and S_b, and the orientations of the two streets before and after deformation, we can determine the components of the deformation gradient by solving the equations,

$$\begin{bmatrix} \cos(\beta) & \sin(\beta) \\ \cos(\Theta+\beta) & \sin(\Theta+\beta) \end{bmatrix} \begin{bmatrix} \frac{\partial x}{\partial X} \\ \frac{\partial x}{\partial Y} \end{bmatrix} = \begin{bmatrix} S_a\cos(\alpha) \\ S_b\cos(\theta+\alpha) \end{bmatrix} \qquad (5a)$$

$$\begin{bmatrix} \cos(\beta) & \sin(\beta) \\ \cos(\Theta+\beta) & \sin(\Theta+\beta) \end{bmatrix} \begin{bmatrix} \frac{\partial x}{\partial X} \\ \frac{\partial x}{\partial Y} \end{bmatrix} = \begin{bmatrix} S_a\sin(\alpha) \\ S_b\sin(\theta+\alpha) \end{bmatrix} \qquad (5b)$$

Specific Problem. Knowing only the angles between, and not the orientations of street segments, and knowing only the pre– and post–deformation strain, the rotation of lines parallel to the maximum extension direction cannot be determined. Thus, we determine only the strains. Without loss of generality, we can reorient the pair of street segments, with the included angle, until street segment a after deformation is parallel to street segment A before deformation (Figure 5C). We select the a (and A) street to be parallel to a coordinate direction that we identify with x (and X) (Figure 5C). In general, street segment b will have a different orientation before and after deformation, according to this procedure. In this way we will be forcing a certain rotation on the system, but we will not become interested in the rotation because it includes an arbitrary component. With this coordinate system, we can complete the determination of the components of the deformation gradient.

In order to explain the method of measuring deformations at an intersection using survey data, consider the NE corner of the intersection of Rinaldi Street and Balboa Boulevard. With the measurements of lengths, we can calculate values of extensions in two directions, the directions parallel to *a* and *b* (Figure 5B). Selecting *a* to be parallel to Rinaldi, we then have two length measurements, *A* for before deformation (in this case, in the 1960's) and *a* for after deformation (in this case, 1994):

$$A = 1320.36 \text{ ft} \tag{6a}$$

$$a = 1320.39 \text{ ft} \tag{6b}$$

and, similarly, along Balboa,

$$B = 177.03 \text{ ft} \tag{6c}$$

$$b = 177.15 \text{ ft} \tag{6d}$$

The resulting *extensions, E*, are,

$$E_a = (a-A)/A = 2 \times 10^{-5} \tag{7a}$$

$$E_b = (b-B)/B = 6.8 \times 10^{-4} \tag{7b}$$

We note two features of these results. First, the extension in the *a*–direction—that is, along Rinaldi—is probably negligible[1], (see Appendix I) because the computed extension is on the order of 10^{-5}. The extension along Balboa is probably significant. Second, both extensions are positive, indicating that both streets lengthened between the times of the measurements.

Thus far we have two measurements of extension, eqs. (7a) and (7b). These provide a component of deformation gradient $(\partial x/\partial X)$ in the *x*–direction and an estimate of the value for the component of deformation gradient $(\partial y/\partial Y)$ in the y–direction (Figure 5C):

$$(\partial x/\partial X) = 1+E_a \tag{8a}$$

$$(\partial y/\partial Y) \cong 1+E_b$$

We will determine the exact value of $(\partial y/\partial Y)$. Examining Figure 5C we see that line segment B has projections *dX* and dY on the axes before, and dx and dy on the axes after deformation, so that,

$$dx = (\partial x/\partial X)dX + (\partial x/\partial Y)dY$$

$$dy = (\partial y/\partial X)dX + (\partial y/\partial Y)dY$$

and, therefore,

$$(b/B)\cos(\theta) = (\partial x/\partial X)\cos(\Theta) + (\partial x/\partial Y)\sin(\Theta) \tag{8b}$$

$$(b/B)\sin(\theta) = (\partial y/\partial X)\cos(\Theta) + (\partial y/\partial Y)\sin(\Theta) \tag{8c}$$

By assumption, however, $(\partial y/\partial X) = 0$, and we know $(\partial x/\partial X)$, so eqs. (8) simplify to

$$(\partial x/\partial Y) = [(b/B)\cos(\theta) - (a/A)\cos(\Theta)]/\sin(\Theta) \tag{9a}$$

$$(\partial y/\partial Y) = (b/B)\sin(\theta)/\sin(\Theta) \tag{9b}$$

$$(\partial x/\partial X) = (a/A) \tag{9c}$$

These results determine the three nonzero components of the deformation gradient.

[1]See Appendix I.

Presentation of Strain State—The Shmoo Extension Figure

Strains have always been very difficult to interpret from maps. The essential problem is that one must be able to display three quantities, such as two sets of contours of strain invariants—for example the maximum and minimum principal strains—plus the directions of the minimum or maximum strains. The directions are commonly shown as trajectories. Such a representation, however, requires three separate maps; consequently, determining the strain state near the same point on each of the maps is cumbersome.

Shmoos and Nerds. We have developed an intuitive way of displaying the state of strain near a point via an extension figure we call a *shmoo*[1]. A special case is a *nerd*. The shmoo or nerd shows, in one diagram, the absolute magnitude of the largest principal strain as well as the directions of the maximum and minimum, principal strains. The extension shmoo is a plot of the extension as a function of orientation.

The extension shmoo is constructed as follows. One element consists of a *larger–extension circle*, the radius of which, ρ, is related to the order of magnitude of principal strains. It is

$$\rho=G(r_o-r)^2;\ r_o \geq r \qquad (10a)$$

in which G is an arbitrary scaling factor, r_o is a cutoff, and r is a measure of the magnitudes of the principal extensions. It is the larger of the relations,

$$r= -\log_{10}[\mathrm{abs}(E_1)] \qquad (10b)$$

or,

$$r= -\log_{10}[\mathrm{abs}(E_2)] \qquad (10c)$$

where the principal extensions[2] are related to the principal strains,

$$E_1=(\varepsilon_1+1)^{(1/2)}-1=[0.5(I_1+(I_1^2-4I_2)^{(1/2)})]^{(1/2)}-1 \qquad (10d)$$

$$E_2=(\varepsilon_2+1)^{(1/2)}-1=[0.5(I_1-(I_1^2-4I_2)^{(1/2)})]^{(1/2)}-1 \qquad (10e)$$

and the invariants are,

$$I_1= (\partial x/\partial X)^2 + (\partial y/\partial Y)^2 + (\partial x/\partial Y)^2 + (\partial y/\partial X)^2 \qquad (10f)$$

$$I_2= [(\partial x/\partial X)\,(\partial y/\partial Y) - (\partial x/\partial Y)\,(\partial y/\partial X)]^2 \qquad (10g)$$

The first invariant, I_1, is a measure of the distortion, and the second invariant, I_2, is equal to the square of the normalized area change. For the Granada Hills survey data (Appendix I), we have determined that extension values smaller in magnitude than 10^{-5} are negligible, so r_o in eq. (10a) is set equal to 5. Then, if r is greater than 5, r is set equal to 5 so that the radius of the circle vanishes to a point. Thus the radius, ρ, of the larger–extension circle of the shmoo is essentially determined by the order of magnitude of the principal extension with the larger absolute value.

For the second element of the shmoo, we plot a radius vector, R, that is determined by the extension in an arbitrary orientation, θ_c,

$$S_c=1+E_c= [(I_2)^{(1/2)}]/[\{(\partial y/\partial Y)\cos(\theta_c)-(\partial x/\partial Y)\sin(\theta_c)\}^2 +\{(\partial x/\partial X)\sin(\theta_c)-(\partial y/\partial X)\cos(\theta_c)\}^2]^{(1/2)} \qquad (11a)$$

[1]We call the extension figure the shmoo, after an object with remarkable properties introduced about 50 years ago in the comic strip, "Li'l Abner

[2]Note that the extension is equal to the strain if the deformations are very small. The deformation is very small if the square of the extension is much smaller than the absolute value of the extension itself.

The radius vector is designed so that it is zero at the larger-extension circle itself:

$$R = \rho(1+E_c\,10^r) \qquad (11b)$$

If the extension, E_c, is positive, the radius vector is larger than ρ so it extends from the center to some distance beyond the larger–extension circle. If the extension is negative (shortening), the radius vector *R* is shorter than ρ, so it is within the larger–extension circle. Note that $E_c\,10^r$ lies between +1 or –1 and ranges to either limit depending on whether the larger extension is positive or negative.

Together, plots of eqs. (10a) and (11b) define the extension shmoos, consisting of a heavy, larger–extension circle and a light, multi–shaped line that commonly has a crude figure–eight shape. If the figure–eight is within the heavy circle, the shmoo becomes a nerd.

Shmoos and nerds graphically display the strain state near a point. The magnitude of the strain is indicated by the radius of the larger–extension circle, which can be compared to a scale of such circles. The directions of the maximum and minimum principal strains correspond to the directions of the maximum and minimum extensions, so the shmoo or nerd indicates the direction of the principal strains.

Finally, one can determine, quantitatively, the amount of extension or compression in any direction by measuring the radius vector, *R*, of a shmoo or nerd and using the relation

$$E_c = [(R/\rho)-1]10^{-r} \qquad (11c)$$

The exponent, *r*, is determined by comparing the radius, ρ, of the larger–extension circle of the shmoo to the scaled strain circles.

The extension shmoos are plotted near the street intersections on the map, (Plate 2).

Appendix II presents the data used to compute the shmoo extension figures. Here *x* is east and *y* is north of the intersection.

Shmoo Language The shmoos are read as follows (please refer to Explanation in Figure 6 or Plate 2): The size of the circle defines the order of magnitude of the strains. To determine the magnitude, the size of the circle is compared to a series of calibrated circles in the Explanation. The circles are for 10^{-1} (= 0.1), $10^{-1.5}$ (≅ 0.03), 10^{-2} (0.01), $10^{-2.5}$ (≅ 0.003) and so forth. Where the multi–shaped line is inside the circle there is compression, and where it is outside the circle there is extension. For example, the shmoo near the intersection of Babbitt and Bircher in Figure 6 shows the multi–shaped, light line is outside the heavy circle, indicating that there is extension in all directions, although the extension is larger in the direction N 45° W. If there is rotation only due to shear parallel to Bircher, then, the maximum extension is in the direction N 45° W, the magnitude of the larger principal strain is on the order of ±0.0006 (between $10^{-3.5}$, 0.0003, and 10^{-3}, 0.001), the principal extensions are positive, and the strains are largely dilational for this example.

The shmoos at the intersection of Halsey and Ruffner show the common, figure–eight shape of the light line, and indicates that there is extension in the NE–SW direction, where the light line is outside the circle, and compression in the NW–SE direction, where the light line is inside the circle. In these examples the magnitude of the larger principal strain is on the order of ±0.002 (between 10^{-3}, 0.001 and $10^{-2.5}$, 0.003). The roughly equal values of maximum shortening and extension in this example suggest shear without area change. Simple shear relative to the orientation of Halsey would be right–lateral. Simple shear relative to the orientation of Ruffner would be conjugate, that is, left–lateral.

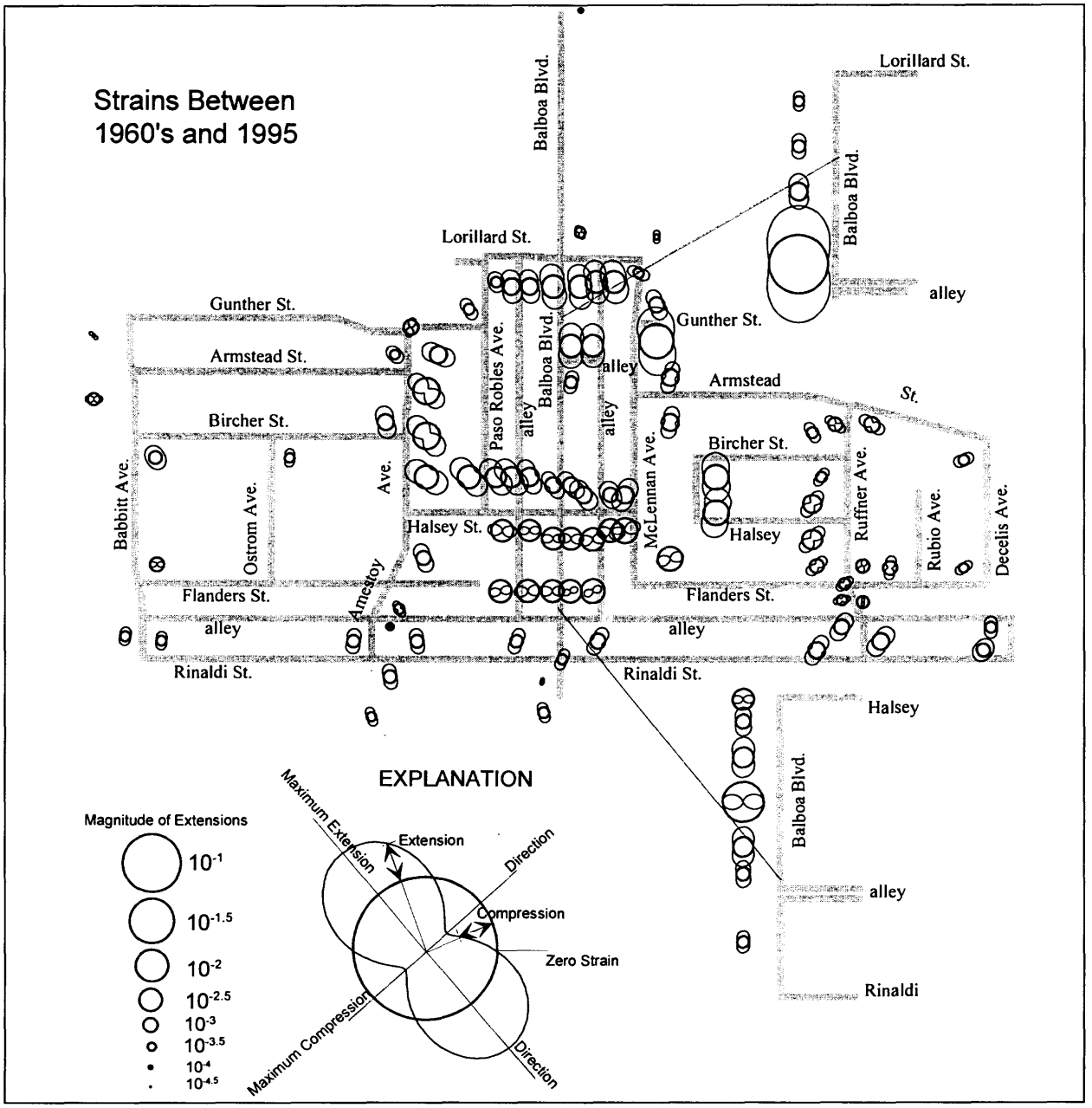

Figure 6. Computed extension figures (shmoos and nerds) for the Balboa Boulevard area of the Granada Hills for the period 1960's–1994. Strains presumably were produced largely during the 1971 San Fernando Valley and 1994 Northridge earthquake sequences. Extension shmoos and nerds represent changes in lengths and angles between street segments at each intersection in the Granada Hills area. The magnitude of the largest extension (regardless of sign) indicated by radius of heavy circle. The magnitude is determined by comparing the size of a circle with the size of calibrated circles, in the Explanation. Thus the circle in the NE quadrant of the intersection of Flanders and Babbitt represents and extension of about 10^{-3}. The circle in the SE quadrant of the intersection of Armstead and McLennan represents an extension of about 10^{-2}. The lighter line of each shmoo represents the distribution of extension in all directions. For the former shmoo (a nerd, actually), there is zero extension east–west and about -10^{-3} extension (compression) north–south. For the latter shmoo, there is zero extension east–west and about 10^{-2} extension north–south.

Thus, the direction of maximum extension (or minimum compression) is defined, to within an unknown rigid–body rotation, by the long dimension of the multi–shaped line. The sense of shear (relative to the east–west or north–south streets) can be read from the inclination of the long dimension of the shmoo.

The shmoo extension figures near the intersection of Lorillard and Balboa in Figure 6 and Plate 2 indicate approximately north–south maximum extension. The magnitude of the larger principal strain is on the order of +0.003 ($10^{-2.5}$). The shearing and east–west compression are essentially zero, although the slight tilting of the long directions of the shmoos suggests a small amount of left–lateral shearing relative to the orientation of Lorillard, (that is, right–lateral shearing relative to Balboa).

Finally, we see examples of nerds south of Halsey Street between Paso Robles and McLennan. The nerd extension figures indicate approximately north–south maximum compression. The magnitude of the larger principal strain is on the order of –0.003 ($-10^{-2.5}$). In some places there is minor east–west extension, and in others this extension is zero. The nerds are horizontal, or slightly turned in a counterclockwise sense, suggesting minor right–lateral shearing relative to Halsey (or left–lateral shearing[1] relative to Balboa).

Distribution of Horizontal Strains

In order to determine the strains in the Granada Hills area we have used the method described above and survey data collected at various times by the City of Los Angeles. Surveys, ranging from partial to complete, were conducted in the 1960's when the subdivisions were originally laid out; in 1972, after the San Fernando earthquake sequence; in 1983; and in 1994–5, after the Northridge earthquake sequence. The resurvey in 1983 was largely limited to the western part of the area and the results are generally uninteresting (Appendix I).

The shmoos are plotted near the corner of the intersection where the data were collected (Figure 6). In many places, however, the shmoos do not represent data highly localized to a street corner, but rather average strains between widely–spaced intersections. For example, the street segments used to compute strains in the north–south direction are generally much longer than those used to compute east–west strains. Thus, north of Halsey and near Balboa the shmoos represent average strains over street segments ranging up to 341 m long in the north–south direction, but only about 107 m, and generally about 55 m long, in the east–west direction. In crucial areas along Balboa, though, we have more detailed information.

Strains During the 1971, San Fernando Earthquake Sequence

Figure 7 shows the shmoo extension figures as determined with surveys conducted in the mid 1960's and in 1972. The magnitudes of the strains are indicated with circles calibrated in the Explanation. We see that the strains are up to an order of magnitude of 10^{-3} within the area. There is right–lateral

[1]Note the different ways of reading sense of shear for shmoos and nerds. The sense for shmoos seems intuitive. That for nerds, then, seems counter-intuitive.

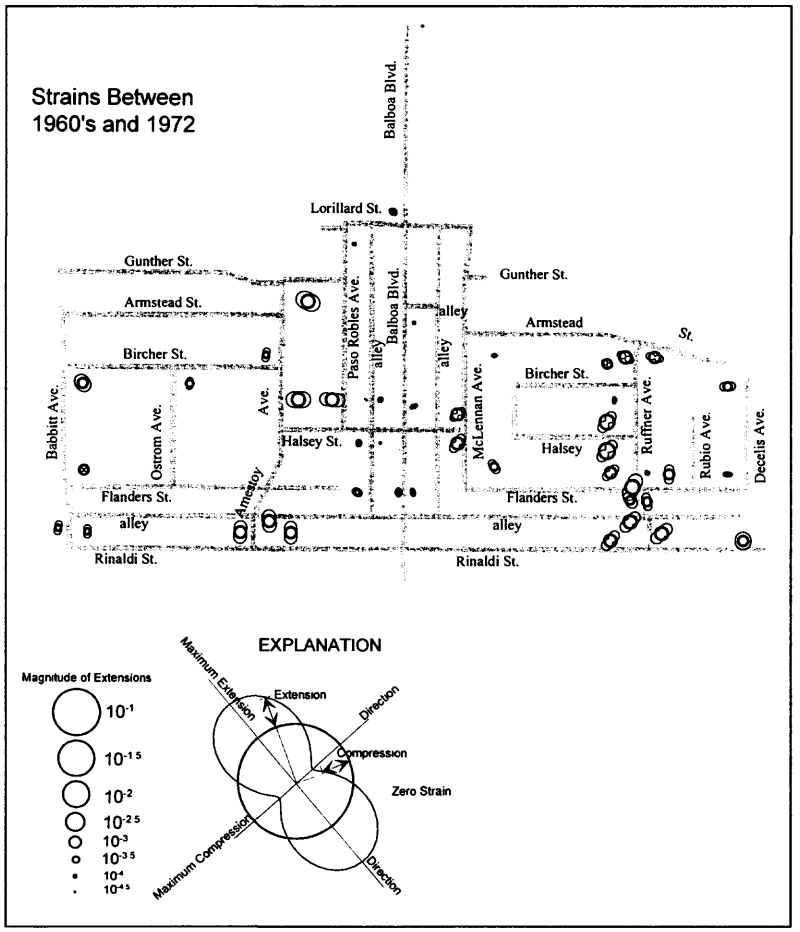

Figure 7. Computed extension figures (shmoos and nerds) for Balboa Street area of Granada Hills for the period 1960's–1972. Strains, if significant, may be a result of the San Fernando earthquake of 1971. The larger extensions are 10^{-3} or smaller throughout the area. The shmoos along Rufner Avenue, south of Bircher, generally indicate left–lateral shearing parallel to Rufner (right–lateral parallel to Rinaldi). If the deformations were due to ground shaking, one probably would expect similar patterns in Figures 7 and 8.

shearing parallel to Flanders, Rinaldi and Halsey, in the eastern part of the area; north–south extension of Amestoy near Rinaldi; and east–west extension of Halsey in the vicinity of Amestoy. It is unclear whether the strains are significant, and there is no obvious pattern.

Strains During the 1994, Northridge Earthquake Sequence

The strains in the Granada Hills area (Figure 8 and Plate 2) associated with the Northridge earthquake sequence form much clearer patterns and are much larger than those associated with the San Fernando earthquake sequence (Figure 7). We used survey data collected in 1983 for reference states for some of the extension figures shown in Figure 7; 1983 data were lacking for most of them, though, so we used 1972 reference states. Note that in Figure 6 we computed strains relative to reference states in the 1960's.

There are three notable features of the pattern of strains in the Granada Hills area shown in Figure 8 and Plate 2. First, the strains in the central part of the area should generally be of significant magnitude. The measurement errors should be on the order of 10^{-5} or $10^{-4.5}$. The calibration circles indicate that such small strains would be represented by dots in the figure. An example is at the upper right end of Balboa. Second, the strains die off to insignificant values on all sides of the area. They are negligible, or at least very small along Babbitt in the west, south of Rinaldi in the south, east of Ruffner in the east, and north of Lorillard in the north. Third, there appear to be three east–west belts of relative-

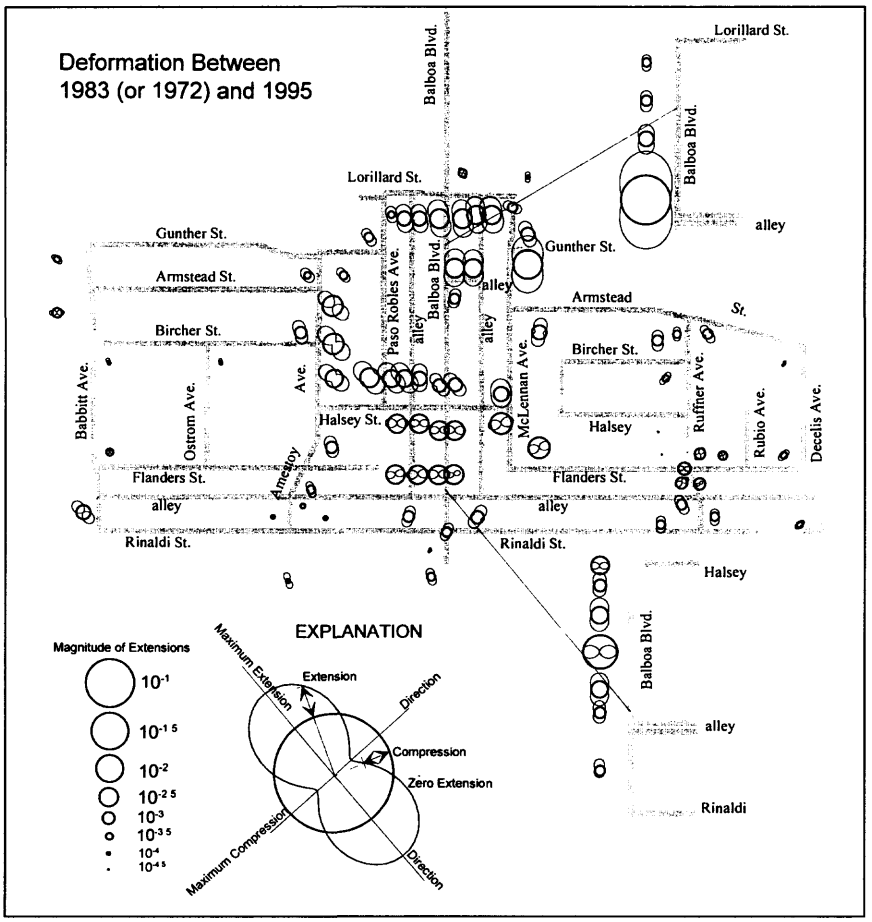

Figure 8. Computed extension figures (shmoos and nerds) for Balboa Street area of Granada Hills for the period 1983 (or 1972) and 1994. The shmoos along Lorillard Street indicate north–south extension on either side of Balboa Boulevard. Those south of Halsey Street and north of Flanders Street, near Balboa, indicate north–south compression. The shmoos north of Halsey Street, near Balboa, and along Amestoy Avenue, between Halsey and Gunther streets indicate left–lateral shearing relative to the orientation of Halsey (or, of course, right–lateral shearing relative to Balboa).

ly homogeneous strain in the area between Amestoy and McLennan (Plate 2). There is a belt of roughly north–south or north–northwesterly extension near Lorillard; the belt may extend as far south as Bircher in the eastern part of the area. A belt of northwest–southeast extension is located north of Halsey and along Amestoy. The third belt, of north–south compression, is south of Halsey and north of the alley north of Rinaldi.

The extension figures show that the strain state along Balboa and several nearby parallel streets was dominated by extension north–south, or about N 10°W, for parts of the streets between Lorillard in the north and Armstead, or the short alley, in the south. A maximum strain of 10^{-2} to 2×10^{-2} was computed for the short cul–de–sac of Gunther that juts eastward from Mclennan, but the strains are generally about $10^{-2.5}$ in that area.

The localized strains along Balboa may be larger than those indicated by the averages determined between intersections. The surveyors measured the widths of lots by measuring distances between "+" marks which the developer had placed in the sidewalks to identify sides of lots. The inset figure in the upper right of Figure 8 shows the north–south extension estimated in this way as a function of position along the sidewalk between Lorillard and the short alley, (note that the shear and east–west extension were *assumed* to be zero for these extension figures). The shmoos indicate that the apparent extensions determined thusly are small, on the order of 0.0003, near Lorillard; that they increase to about 0.003 southward, half–way

along Balboa; and then suddenly increase to about .025 m in a 3.35 m expanse of sidewalk just north of the alley, (width of 3.048 m before and 3.362 m after earthquake sequence).

Assuming the measurements of apparent extension in the sidewalk reflect those one would make with monuments at depth, one would conclude that the strains in the ground are highly concentrated. This may well be correct, and this assumption is supported by the observation that the gas and water mains broke in Balboa in the vicinity of the 3.4 m section with the large apparent strain (Plate 2). Conversely, deformations and fracturing of sidewalks, roads, and house foundations provide notoriously–poor estimates of deformations in the ground beneath such structures, as we saw at Loma Prieta, (Martosudarmo and others, unpublished data). For this reason, we do not mix the data collected from measurements in the sidewalk (inset figure in upper and lower right of Figure 8) with measurements collected by surveying center–line monuments.

The belt of north–south extension in the northern part of the area is separated from a belt of north–south compression, south of Halsey and north of Rinaldi, by a belt of north–south extension and east–west, left–lateral shearing north of Halsey.

South of this belt is the belt of north–south compression, with nerds characterized by a circle with a figure–eight–shaped, thin line inside. The average magnitude of the compression is about –0.003. The surveyors also measured the widths of lots (as described above) along Balboa between Halsey and Rinaldi. Their measurements are shown with shmoos in the lower inset diagram of Figure 8. The diagram shows that there is generally *extension* in the sidewalk, except in one lot where there is high compression, (width of 18.288 m before and 17.880 m after earthquake sequence). This result is fascinating because it suggests that the compression is extremely–highly localized. As indicated above, though, one cannot depend on details of fracturing and deformation in surficial structures to infer strains at depth. We regretfully conclude that the compression occurs over an unknown length of Balboa between Halsey and the alley north of Rinaldi.

Figure 9 shows the extension figures in relation to the positions of known or suspected faults in the Granada Hills area (Figure 4). The Mission Hills fault is close to Index Street, south of Rinaldi, where the large gradient in change in altitude occurs. It also cuts through the area near Rinaldi and Amestoy. It might well extend through the center of the area, because its trace is inferred. The dip of the Mission Hills fault toward the north and the upthrown north side are consistent with the pattern of an east–west band of extension parallel to an east–west band of compression.

Length Changes Along Balboa

The possible causes for the deformation in the Granada Hills area can be constrained through comparison of strains calculated along Balboa to the differential displacements and to the cumulative differential displacements of the two ends of each street segment. For this purpose we arbitrarily fix the intersection of Balboa and Midwood, which is about 335 m north of Rinaldi, assuming that it did not move. Then we compute the values given in Table 1. Note that there is a small compression of the street between Midwood and Lorillard, (both the 106 and 235 m sections of this road were shortened). There were large extensions between Lorrillard and the short alley, and between the short alley and Halsey. We see that in these two sections there was a total of 0.515 m of extension, and only 0.314 m of this was highly localized in the 3.35 m section of sidewalk, so the extension was certainly not localized on a single

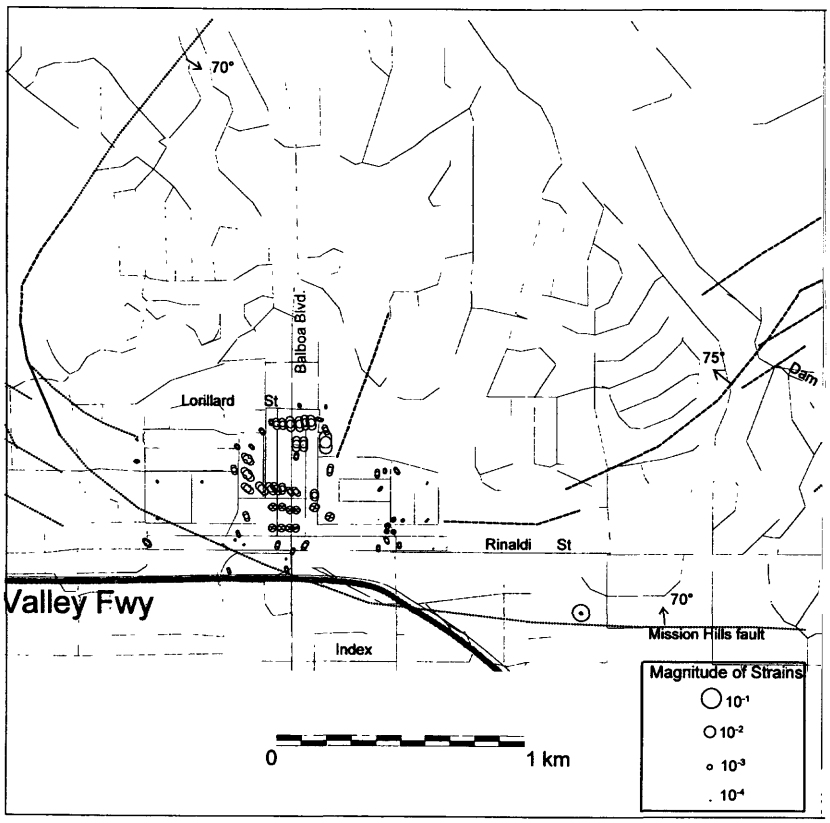

Figure 9. Pattern of shmoos and nerds compared to traces of known or suspected faults in the Granada Hills area. The Mission Hills fault has an orientation and downthrown side consistent with the pattern of surface extensions. Perhaps the trace of the fault is through the middle of the Granada Hills area rather than at the south and eastern edges, as shown here.

fracture at depth. Table 1 shows that about 0.427 m of compression occurred between Halsey and the alley north of Rinaldi. We noted above that, of this, 0.408 m of compression was measured in the sidewalk of a single lot, indicating the highly–localized compression in that sidewalk. Although this does not necessarily mean that the compression at depth was so highly localized, water and gas pipelines were ruptured in compression at the site where high compression of the sidewalk was measured, as shown in Plate 2.

Table 1 shows that, within the length extending over a horizontal distance of about 928 m, from near Midwood Street about 335 m north of Lorillard, to the alley south of Rinaldi, and near the right–of–way of the Simi Valley Freeway (Plate 2), the net change in length was only about 0.15 m, which corresponds to an average strain of about 2×10^{-4}. Note that strains of this magnitude are essentially negligible in Figure 8 and Plate 2. As explained in Appendix I, we expect strains smaller than 10^{-4} to be negligible. Thus, the average strain is negligible.

The table also shows that the pattern of length changes from north to south consists of a negligible amount of shortening (0.006 m; average strain of -2×10^{-5}), adjacent to a broad zone of lengthening (0.515 m; average strain of 1.5×10^{-3}), adjacent to a broad zone of compression (0.427 m; average strain of -3×10^{-3}), which is, in turn, adjacent to a narrow zone of lengthening (0.061 m; 6×10^{-4}).

Thus, any model one wants to suggest for the pattern of strains, and for the patterns of differential displacements, needs to account for both the pattern of strains and the small net change in length.

Table 1. Changes of Length of Balboa Boulevard between Intersections

(All measurements in meters)

Cross Street	Street Length	Length Change	Cumulative Change
Midwood	0		
Lorillard	342.251	–0.006	–0.006
short alley	133.003	0.399	0.393
Halsey	203.399	0.116	0.509
alley	140.775	–0.427	0.082
Rinaldi	53.959	0.037	0.119
alley	54.888	0.024	0.143

Changes in Altitude

In Plate 1 we showed contours of differential vertical uplift in the San Fernando Valley; earlier, we discussed the general, fan–shaped pattern, and four areas of disturbance, including an area in Granada Hills. Table 2 and Figure 10 show further details of altitude changes in the Granada Hills area, the focus of the present study.

Profiles of altitude changes along the two streets are shown in Figure 10, with the heavy line for Balboa and the light line for Rinaldi. The profile to the south (left) of that shown for Balboa is a relatively–uniform gradient across the valley. North of San Fernando Mission Boulevard, at Index Street, the altitude drops about 0.12 m[1]; it then increases from about 0.21 m at Index Street, just south of Simi–Valley Freeway, to about 0.45 at Woodley Avenue; there it peaks, then drops to about 0.4 m, roughly 2 km farther north. The profile west on Rinaldi is similar to the profile north on Balboa, indicating that the principal gradient is northwestward, as Plate 1 shows.

Of course, we do not know the causes of the strains and differential vertical displacements in the Rinaldi/Balboa area of San Fernando Valley. We suspect that the general uplift, represented by overall tilting (shown in Figure 10 and visible in Plate 1) is a result of a listric fault, with positive curvature that slipped during the main shock, the numerous aftershocks and, presumably, also during creep associated with the 1994 earthquake sequence. On the basis of the study reported thus far, we tentatively suggest that the local perturbation of the fan–shaped gradient, expressed in the increase in gradient northwest and the decrease of gradient southeast of the intersection of Balboa and Rinaldi, reflects slip on a small, near–surface, blind reverse fault or shear zone, dipping steeply northwestward beneath the Santa Susana Mountains. As such, this blind reverse fault apparently was coactive with movement on the curved fault that produced the main shock of the earthquake sequence.

[1]We seriously questioned this measurement because it was so different from those of nearby monuments. Robert Jones, Surveyor, City of Los Angeles, however, rechecked the calculations and releveled the position of the benchmark at Index Street, and indicated that he obtained the same value, to within the error of the instrument. Furthermore, he inspected the area of the benchmark and found no evidence of disturbance.

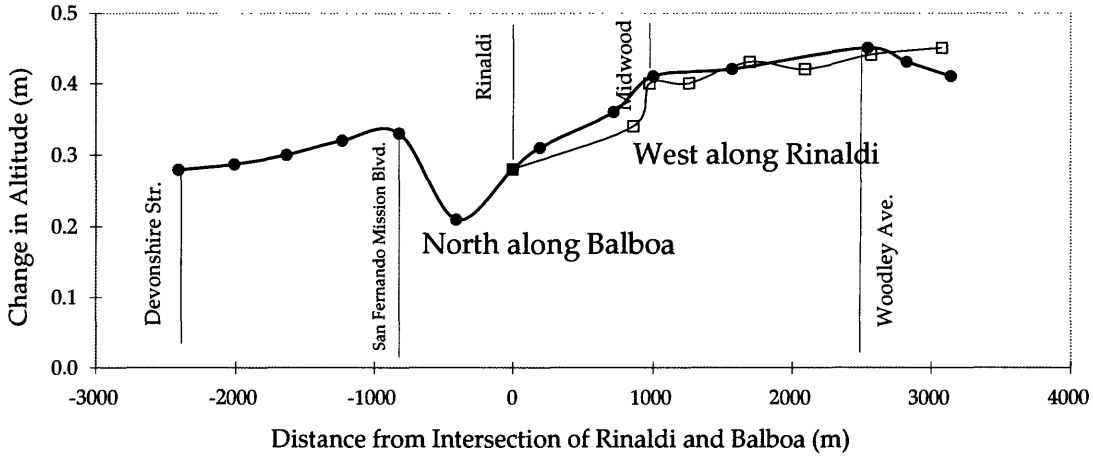

Figure 10. Changes of altitude with north–south distance along Balboa Boulevard and with east–west distance along Rinaldi. The Granada Hills area is between Rinaldi and Midwood along Balboa. The low is at Index Street. The overall tilting of the area is about 0.45 m at Woodley, minus 0.28 m at Devonshire, over a horizontal distance of about 5000 m.

Table 2. Changes in Altitude of Some Street Intersections in Granada Hills Area

Cross Street	Distance from Rinaldi	Altitude Change
North Along Balboa		
	(m)	(m)
	3141.03	0.41
	2820.51	0.43
	2538.46	0.45
	1564.10	0.42
Midwood	1000.00	0.41
Lorillard	717.95	0.36
Halsey	192.31	0.31
Rinaldi	0.00	0.28
Index	–410.26	0.21
San Fern.	–820.51	0.33
Tulsa	–1230.77	0.32
West Along Rinaldi		
Balboa	0.00	0.28
Babbitt	858.97	0.34
Lasaire	974.36	0.40
	1256.41	0.40
White	1692.31	0.43
Zelzan	2089.74	0.42
	2564.10	0.44
	3076.92	0.45

Fractures and Damage to Structures

Hecker and others (1995a) have published an aerial–photograph map of fractures and damage to houses, sidewalks, and roads that occurred in the Granada Hills and Mission Hills areas during the Northridge earthquake sequence. Plate 3 is a slightly simplified rendition of the cracks in the Bull Canyon area in Granada Hills, put on a scaled base of roads and topography. Only in a few places did we add cracks based on our own observations.

The cracks and damage to houses are highly concentrated in the central part of the area. Presumably, the damage to houses is a result of permanent ground deformation. It is possible, however, that this damage could be associated with more–intense shaking that is related in some way to the permanent ground deformation. To establish an association between damage to streets and permanent ground deformation, it is necessary to show that the kinematics of deformation accommodated by fracturing in the streets is the same as that of the ground. We can do this by comparing the patterns of superficial fractures mapped by Hecker and others (1995a) with the patterns of strains determined by resurveying street monuments. While this comparison cannot show that the destruction of houses is caused by permanent ground deformation, rather than by shaking alone, such a cause is suggested in Plate 3, which shows that damaged and destroyed houses here are largely restricted to the areas of ground fracturing.

Just as at Loma Prieta—where one needed to investigate the kinematic features in order to separate cracks associated with ground lurching (in some cases possible landslide blocks) from those associated with throughgoing tectonic features (Aydin and others, 1992; Johnson and Fleming, 1993; Martosudarmo and others, 1996) at Granada Hills one must distinguish fracturing associated with man–made fill, or the walls of Bull Canyon or the Simi Valley Freeway, with cracks associated with throughgoing tectonic features.

Fractures Associated with Localized Mass Movement

The cracks and thrusts within the connecting street between Rinaldi and Halsey, between Hayvenhurst and Gothic (Plate 3), in the eastern part of the area, are associated with man–made fill placed in the early 1970's, over the old valley of Bull Canyon. These probably are a result of ground shaking and settlement. The cracks within and immediately adjacent to Bull Canyon, north of the filled area, presumably are a result of lurching or, in some cases, sliding of ground adjacent to the steep western wall of Bull Canyon. There are lurching cracks, or cracks defining the headscarp of a landslide mass, about 120 m wide in the east–west and 90 m wide in the north–south direction—along the southern wall of Bull Canyon immediately north of Rinaldi at Hayvenhurst. All of these cracks appear to be associated with relatively superficial ground movement.

Fractures of Uncertain Origin

There are a few other crack patterns that are of less certain origin. The arcuate pattern of tension cracks, defining a graben, parallel to the east side of Ruffner, at Halsey, could be related to a superficial ground movement, such as a slide. The energetics, however, suggested by the arcuate pattern, and the vector of differential displacement measured by Hecker and others (1995), do not make sense in terms of superficial ground movement. The graben would bound a mass that moved southeastward. The problem is that the stream bank that would have provid-

ed the maximum sliding potential is about 210 m *northeastward* from the graben, nearly at right angles to the vector of differential displacement. Another short arcuate pattern that may define a graben of a slide mass is between Armstead and Bircher and between Ruffner and McLennan. Again, the energetics of movement do not make sense in terms of sliding. The sliding mass would have been on the southeast side of the graben and would have moved in a southeasterly direction. The closest stream bank is 60 to 90 m *north* of the graben.

There are only a very few cracks in the western part of the area, along Babbitt and Louise.

Fractures of Tectonic Origin

We suggest that most of the remaining fractures are of tectonic origin. They appear to define two belts (Plate 3). One belt, about 60 m wide, extends from the wall of Bull Canyon, immediately northeast of the small cul–de–sac of Gunther (north of Armstead), south–southwest about 460 m, to the intersection of Amestoy and Bircher. This belt is dominated by tension cracks, grabens, and small normal faults. The southern limit of the eastern part of the belt might be the area of tension cracks at the sharp corner in Bircher, southeast of the intersection of Armstead and McLennan.

The other belt is dominated by compression features, including some thrusts. It is about 120 m wide and extends 800 m, from the intersection of Decellis and Flanders, east–west between Halsey and Flanders, to the intersection of Flanders and Amestoy.

Comparison of Fracture and Strain Patterns

In Plate 2 we have superposed the shmoo extension figures shown in Figure 8 on the map of fractures shown in Plate 3, but without the topographic contours and damaged houses. We note that the strains are negligible, or unmeasurable, in the areas near fractures that are almost certainly related to mass movement of fills or ground immediately adjacent to the bank of Bull Canyon and the cut slope of Simi Valley Freeway. The strains are also very small in the area of the arcuate, graben structure east of Ruffner, which we consider to be of uncertain origin. The belt of relatively large north–south extension coincides with the belt of tension cracks and normal fractures, and the belt of relatively large north–south compression coincides with the belt of thrusts and compression features mapped by Hecker and others (1995a). Thus the types, orientations and positions of superficial fractures in sidewalks, pavement and the ground surface closely correspond with the signs and orientations of the strains calculated from measurements of the center–line monuments. This correspondence strongly supports a conclusion that the localized strains are responsible for the fracturing we have interpreted to be of tectonic origin.

We also suggest that the strong correlation between the damage to houses and the incidence of ground fracturing, shown in Plate 3, indicates that the high concentration of damage or destruction of houses is also a result of the localized strains and, therefore, a result of tectonic deformation, not ground shaking.

A Model for the Deformations

Conceptual Model

As suggested by examination of the pattern of contours of vertical differential uplift in the San Fernando Valley, we propose that, during the Northridge sequence of earthquakes, there were one or more coactive faults or shear zones in the subsurface beneath Granada Hills. In particular, we suggest that:

(1) Most of the fracturing and ground deformation in the Granada Hills area is a result of that coactive faulting or localized shearing.

(2) Fault slip terminated at some depth below the surface.

(3) The surface deformation reflects strains near the ground surface produced by fault slip or localized shearing below.

According to this conceptual model, the ground deformation is associated not only with a blind fault, but also a blind fault blade. The width of the fault in the east–west direction, then, is on the order of the widths of the belts of fracturing, 1,500 to 2,500 m. Fault blades or segments are typical of faults (for example, Plafker, 1971; Clark, 1972; Fleming and Johnson, 1989; Wallace, 1990; Scholz, 1990; Zhao and Johnson, 1992; Crone and others, 1992). The faults that ruptured during the nearby, 1971 San Fernando earthquake were also characteristically blades (e.g., Saul, 1974; Sharp, 1974, fig. 2).

Theoretical Model

We have performed a theoretical analysis of an idealized conceptual model that will provide information we can compare qualitatively to observations. We use a boundary–element model, discussed elsewhere (Wei and Johnson, 1996, in prep.), which can be used to study folds formed as a result of large deformation on a fault in a flowing material, or to study displacements and strains formed as a result of unloading of a fault in linear elastic material. In either case, the material is incompressible (Poisson's ratio is 0.5 for elastic material), so the sections are balanced. The model is the same as that used to study the form of the heart structure underlying San Fernando Valley (Figure 3).

First we examine the general pattern of fold development in passive layering that results from slip on a blind fault in a flowing medium that is shortening overall. Figure 11 shows two steps in the formation of structures in planar bedding (passive markers) as a result of slip on a blind reverse fault at depth at extensions corresponding to E = –0.05 (5%) and –0.01 (10%). The reverse fault is initially inclined at 45° but, of course, it steepens as overall shortening occurs. The formation of an anticline—one so asymmetric that it is essentially a monoclinal fold—above the tip of the blind fault is as expected intuitively. The "reverse drag" on layers at depth, along the fault, is perhaps nonintuitive, but is a result of easy slippage on the theoretical fault, as explained by Wei and Johnson (1996, in prep.). The deformation pattern associated with a normal fault, according to the same model, is shown in Figure 12. A synclinal monocline forms over the tip of the fault, near the ground surface, and the fold pattern, including the depression in the ground surface, is as expected.

Although the models shown in Figures 11 and 12 are patterns one would expect as a result of long–term shortening, we would expect a different pattern of deformation as a result of a single earthquake sequence. In the case of the Northridge earthquake, the coordinates are determined shortly before and

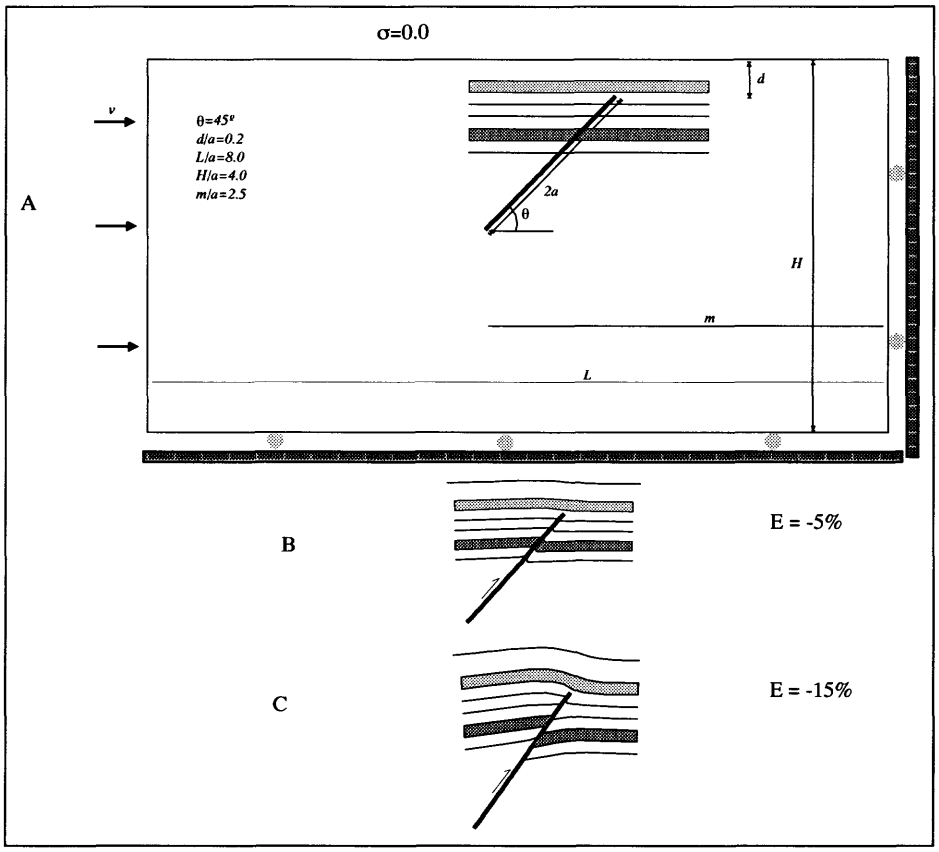

Figure 11. Formation of a faulted fold in compression of a flowing material containing a blind reverse fault (after Wei and Johnson, 1996, in prep.). Layers are passive. The medium is incompressible, so the section is balanced. The system is shortened horizontally and thickens vertically, causing the fault to slip. The result is an asymmetric anticlinal fold above the termination of the reverse fault.

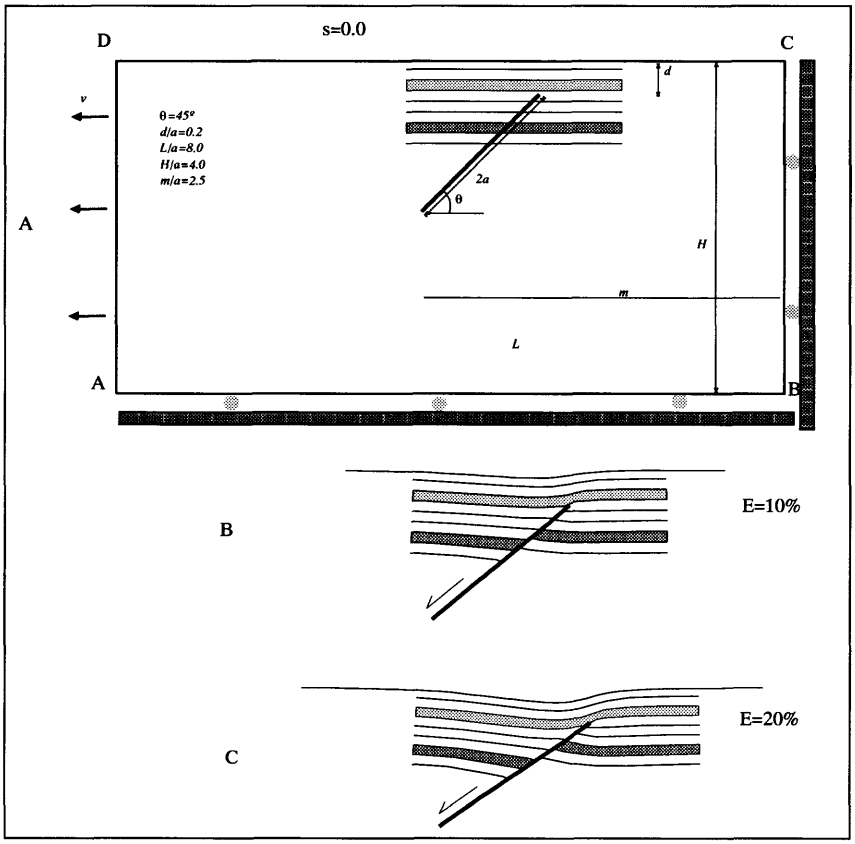

Figure 12. Formation of a faulted fold in extension of a flowing material containing a blind normal fault (after Wei and Johnson, 1996, in prep.). Layers are passive. The system is lengthened horizontally and thins vertically, causing the fault to slip. The result is an asymmetric synclinal fold above the termination of the reverse fault.

shortly after the earthquake, so we would expect to see unloading along a fault. We can, however, use the same surface–element model to analyze the deformation during unloading in order to determine the pattern of differential displacements and strains resulting from the stress drop. We compare initial and final lengths of line segments at the ground surface to determine the normal strains of surface elements. It is this strain distribution that we can compare, qualitatively, to the strains determined at intersections measured by surveying.

Figure 13A shows vertical displacement of the ground surface and distribution of extension parallel to the ground surface for unloading of a fault originally under compression, and with a dip of 45°. Both the vertical displacement and the strains are highly exaggerated, but the patterns are legitimate. For a reverse fault, there is a broad zone of surface–parallel compression near the tip and to the right of the fault tip. There is a large peak of compression to the right and a lower peak of extension to the left of the fault tip (Figure 13A). For a more–steeply–dipping reverse fault, the magnitudes of peaks of extension and compression become more nearly equal, as indicated in Figure 13B for a fault dipping 60°.

Surface displacement and extension distributions for reverse and normal faults are compared in Figure 14. The symmetry of the shape of the deformed ground surface and the distribution of strains are as expected: a strong compression peak for reverse faulting and a strong extension peak for normal faulting.

The results of the theoretical analysis of slip on a blind fault can be applied qualitatively to the results of the measurements of deformation and displacement in the Granada Hills area. We see from the theoretical analysis that, for slip on a steep, blind fault, there should be an area of extension next to an area of compression. This we see, of course, in both the pattern of fractures and in the pattern of strains (Plate 2). The patterns of surface–parallel extensions derived for faults dipping 45° and 60° suggest that the pattern of strains in the Granada Hills is consistent with a fault dipping more steeply than 45° and, perhaps, even more steeply than 60°. Because the fault is steep, one would not be able to determine, with the strain pattern, whether the fault is normal or reverse. The patterns would be essentially the same unless the faults dip relatively gently, as shown (in Figure 13) for faults dipping 45°.

Discussion

In our investigation of the Granada Hills area we have examined the fractures in the field, the map of fractures by Hecker and others (1995a), and the deformational patterns determined with survey data collected by the City of Los Angeles. We have developed and implemented a method of strain analysis using such survey data, and have performed theoretical analyses of a mechanical model of a reverse fault near a free surface that appear to be relevant to our understanding of the field situation. Taken together, these methods provide strong circumstantial evidence that a fault blade beneath the Granada Hills area moved coactively with the faults that produced the Northridge earthquake sequence. Furthermore, we can show, from pre– and post–1971 survey data, that this blade did not move during the San Fernando earthquake sequence.

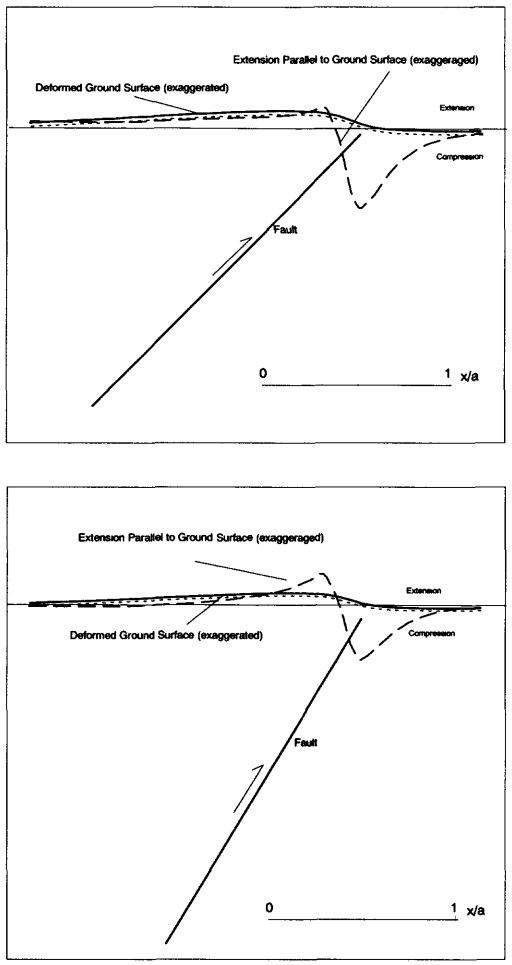

◀ *Figure 13. Distributions of change in altitude and surface–parallel extension of deformed ground surface (highly exaggerated) above blind reverse faults that have unloaded elastically as a result of slip on the fault. A. Reverse fault dipping at 45°. The position of the tip of the fault is shown correctly, relative to the length of the fault, below the horizontal line which represents the ground surface to scale. The surface form (not to scale) shown for the deformed ground surface is asymmetrical and essentially monoclinal. The distribution of extensions shows a narrow zone of high extension behind the tip of the fault and a deep trough of compression over the tip and in front of the tip of the fault. B. Reverse fault dipping more steeply, at 60°. The peak of extension behind the tip and the trough of compression in front of the tip are more nearly the same magnitude.*

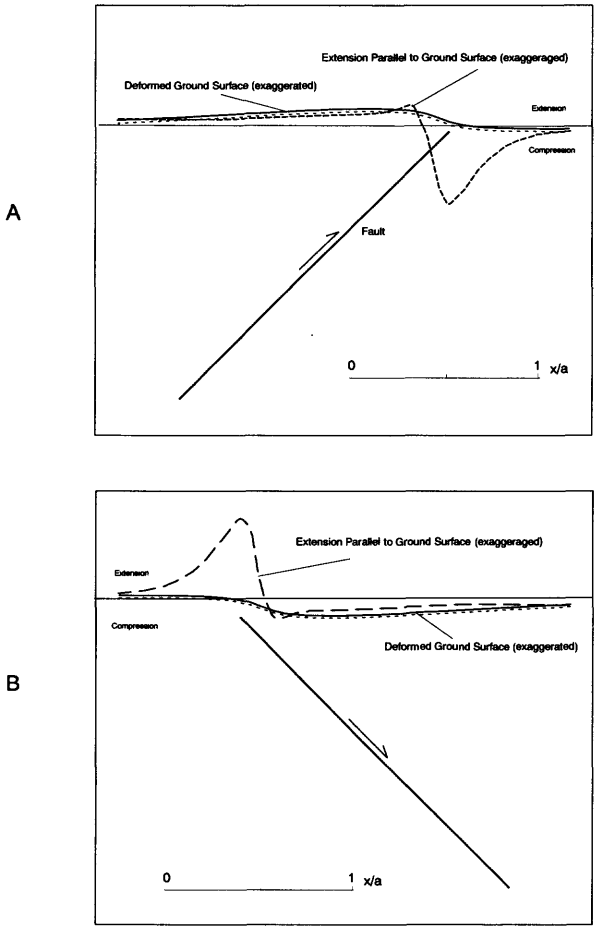

▶ *Figure 14. Distributions of change in altitude and surface–parallel extension of deformed ground surface (highly exaggerated) above blind reverse and normal faults that have unloaded elastically as a result of slip on the fault. A. Reverse fault dipping at 45°. Same as Figure 13A. B. Normal fault dipping at 45°. The position of the tip of the fault is shown correctly, relative to the length of the fault, below the horizontal line that represents the ground surface to scale. The synclinal form of the surface (not to scale) is strongly asymmetrical and essentially monoclinal. The distribution of extensions is analogous to that for the reverse fault, but with a deep trough of extension over and behind the tip and a small trough of compression in front of the tip of the fault.*

Although it is well known that faults appear as blades rather than continuous surfaces, we are surprised that the inferred fault blade in the Granada Hills is so narrow, extending only about 500 m in an east-west direction.

Our study has resulted in conclusions different from those, based on a thorough study of fractures in superficial materials, drawn by Hecker and others (1995a, 1995b). Briefly, these authors conclude that ". . . Small–displacement cracks comprise discrete zones with characteristics that reflect control by local physiographic and near–surface conditions...This set of observations points to shallow mass movement, perhaps in conjunction with compaction, as the cause of deformation in the [Granada Hills] area west of Bull Canyon" [Op. Cit., p. 1]. Holzer and others (1996) draw the same conclusions. Certainly, some of the fractures in the Granada Hills area result from near–surface, superficial phenomena. Many of the fractures in the vicinity of Bull Canyon probably are a result of a combination of ground shaking and the occurrence of the free face of the west bank of Bull Canyon at the eastern edge of the area. Curiously, though, there are very few cracks that appear to be related to the steep, northern cut of the Simi Valley Freeway, at the southern edge of the area, and there is no deformation of the Balboa Boulevard bridge that crosses the freeway. Furthermore, while the 500-m-extent of the consistent pattern of deformation might appear to be narrow for a fault blade, it would be very wide for the local physiographic conditions to control the deformation.

Circumstantial evidence developed in our investigation leads us to the conclusion that the primary mechanism for deformation in the Granada Hills area is permanent ground deformation resulting from movement on a blind fault or shear zone below. The regularities of belts of extension features and compression features, which Hecker and others (1995a, 1995b) mapped (shown in Plate 3), and a very similar pattern of extension figures based on measurements of length and angle changes between centerline monuments (Plate 2), suggest a deep–seated feature. The combination of the belts of extension and compression features with a pattern of steepening of the contours of differential vertical uplift in the vicinity of Granada Hills (Plate 1 and Figure 6) provides even stronger evidence that the permanent ground deformation is a result of deep–seated faulting.

Our research at Granada Hills supports a growing body of evidence that any active fault approaching the ground surface, or cutting the surface in an area has the potential of moving coactively at the time of a major earthquake sequence in that area. This movement can cause localized ground deformation and, therefore, localized damage to structures, utilities, highways, and other lifelines. It is clearly unjustified to assume that intense ground deformation during an earthquake sequence will be restricted to a band a few meters wide (e.g., Hart, 1992; Holzer, 1994), or even a belt a few hundred meters wide (Johnson and Fleming, 1993; Johnson and others, 1994) along the trace of the fault that produced the main shock of an earthquake sequence.

References Cited

Allen, C.R., Wyss, M., Brune, J.N., Grantz, A., and Wallace, R., 1972, Displacements on the Imperial, Superstition Hills, and San Andreas faults triggered by the Borrego Mountain earthquake: United States Geological Survey Professional Paper 787, p. 87-104.

Aydin, A., Johnson, A.M., and Fleming, R.W., 1992, Right-lateral-reverse surface rupture along the San Andreas and Sargent faults associated with the October 17, 1989, Loma Prieta, California, earthquake: Geology, v. 20, no. 12, p. 1963-1967.

Barnhart, J.T., and Slosson, J.E., 1973, The Northridge Hills and associated faults—A zone of high seismic probability?, *in* Moran, D.E., Slosson, J.E., Stone, R.O., and Yelverton, C.A., eds., Geology, seismicity, and environmental impact: Los Angeles, California, University Publishers, p. 253-256.

Barrows, A.G., Kahle, J.E., Saul, R.G., and Webert, Jr., F.H., 1974, Geologic map of the San Fernando earthquake area: California Department of Conservation, Division of Mines and Geology Bulletin 196, plate 2.

Clark, M.M., 1972. Surface rupture along the Coyote Creek fault: United States Geological Survey Professional Paper 787, p. 55-86.

Crone, A.J., Machette, M., and Bowman, J.R., 1992, Geologic investigations of the 1988 Tennant Creek, Australia, Earthquakes – Implications for paleoseismicity in stable continental regions: United States Geological Survey Professional Paper 2032-A, 51 p.

Davis, T.L., and Namson, J.S., 1994, A balanced cross-section of the 1994 Northridge earthquake, southern California: Nature, v. 372, p. 167-169.

Fleming, R.W., and Johnson, A.M., 1989, Structures associated with strike-slip faults that bound landslide elements: Engineering Geology, v. 27, p. 39-114.

Haegerud, R.A., and Ellen, S.D., 1990, Coseismic ground deformation along the northeast margin of the Santa Cruz Mountains, Field guide to the neotectonics of the San Andreas fault system, Santa Cruz Mountains, in light of the 1989 Loma Prieta earthquake: United States Geological Survey Open File Report 90-274, 32-36 p.

Hart, E.W., 1992, Fault-rupture hazard zones in California: California Department of Conservation, Division of Mines and Geology, Special Report 42, p. 1-26.

Hauksson, E., Jones, L.M., and Hutton, K., 1995. The 1994 Northridge earthquake sequence in California: Seismological and tectonic aspects: Journal of Geophysical Research, v. 100, p. 12,335-12,355.

Hecker, S., Ponti, D.J., Garvin, C.D., Powers, T.J., Fumal, T.E., Hamilton, J.C., Sharp, R.V., Rymer, M.J., Prentice, C.S., and Cinti, F.R., 1995a, Ground deformation in Granada Hills and Mission Hills resulting from the January 17, 1994, Northridge, California, earthquake: United States Geological Survey Open-File Report 95-62, 11 p.

Hecker, S., Ponti, D.J., Garvin, C.D., Hamilton, J.C., Sharp, R.V., Rymer, M.J., Prentice, C.S., and Cinti, F.R., 1995b, Characteristics and origin of ground deformation produced in Granada Hills and Mission Hills resulting from the January 17, 1994, Northridge, California, earthquake, *in* Seiple, R., and Woods, M., eds., Northridge Earthquake: California Department of Conservation, Division of Mines and Geology Special Publication.

Holzer, T.L., 1994, Loma Prieta damage largely attributed to enhanced ground shaking: Eos, v. 75, p. 299-301

Hudnut, K.W., Shen, Z., Murray, M., McClusky, S., King, R., Herring, T., Hager, T., Feng, Y., Fang, P., Donnellan, A., and Bock, Y., 1996, Co-seismic displacements of the 1994 Northridge, California, earthquake: Bulletin of the Seismological Society of America, v. 86, n. 1B. p. S19-S36.

Jennings, C.W., 1973, State of California, Preliminary fault and geologic map, south half. Scale 1:750000: California Department of Conservation, California Division of Mines and Geology Preliminary Report 13.

Johnson, A.M., and Fleming, R.W., 1993, Formation of left-lateral fractures within the Summit Ridge shear zone, 1989 Loma Prieta, California, earthquake: Journal of Geophysical Research, v. 98, p. 21,823-21,837.

Johnson, A.M., and Fletcher, R.C., 1994, Folding of viscous layers: New York, New York, Columbia University Press, 461 p.

Johnson, A.M., and Pollard, D.D., in prep. Principles and Practice of Structural Geology. Prentice-Hall.

Johnson, A.M., Fleming, R.W., and Cruikshank, K.M., 1993, Broad belts of shear zones as the common form of surface rupture produced by the 28 June 1992 Landers, California, earthquake: United States Geological Survey Open-File Report 93-348, 61 p.

Johnson, A.M., Fleming, R.W., and Cruikshank, K.M., 1994, Shear zones formed along long, straight traces of fault zones during the 28 June 1992 Landers, California, Earthquake: Bulletin of the Seismological Society of America, v. 84, no. 3, p. 499-510.

Lazarte, C.A., Bray, J.D., Johnson, A.M., and Lemmer, R.E., 1994, Surface breakage of the 1992 Landers earthquake and its effects on structures: Bulletin of the Seismological Society of America, v. 84, no. 3, p. 547-561.

Malvern, L.E., 1969, Introduction to the mechanics of continuous medium: Englewood Cliffs, New Jersey, Prentice-Hall, Inc., 713 p.

Moffitt, F.H., and Bouchard, H., 1992, Surveying: New York, New York, Harper Collins, 848 p.

Oakshott, G.B., 1958, Geology and mineral deposits of the San Fernando quadrangle, Los Angeles County, California: California Department of Conservation, California Division of Mines and Geology Bulletin 172, 147 p.

Plafker, G., 1966, Surface faults on Montague Island: United States Geological Survey Professional paper 543G, 42 p.

Plafker, G., and Galloway, J.P., 1989, Lessons learned from the Loma Prieta, California, Earthquake of October 17, 1989: United States Geological Survey Circular 1045, 48 p.

Ponti, D.J., and Wells, R.E., 1991, Off-fault ground ruptures in the Santa Cruz Mountains, California: Ridge-top spreading versus tectonic extension during the 1989 Loma Prieta earthquake: Bulletin of the Seismological Society of America, v. 81, p. 1408-1510.

Saul, R.B., 1974, Geology of the southeast slope of the Santa Susana Mountains and geologic effects of the San Fernando earthquake: California Department of Conservation, California Division of Mines and Geology Bulletin 196, p. 53-70.

Scholz, C.H., 1990, The mechanics of earthquakes and faulting: Cambridge, Cambridge University Press, 439 p.

Sharp, R.V., 1974, Displacement on tectonic ruptures: California Department of Conservation, California Division of Mines and Geology Bulletin 196, p. 187-194

Shen, Z.K., Ge, B.X., Jackson, D.D., Potter, D., Cline, M., and Sung, L.Y., 1996, Northridge earthquake rupture models based on the global positioning system measurements: Bulletin of the Seismological Society of America, v. 86, p. 537-548.

Stone, D.S., 1996, Structural trend analysis by axial surface mapping: Discussion: Bulletin of the American Association of Petroleum Geologists, v. 80, p. 770-779.

Tada, H., Paris, P.C., and Irwin, G.R., 1985, The stress analysis of cracks handbook, Second Edition: Del Research Corp., Hellertown, Pennsylvania.

U.S. Geological Survey Staff, 1990, The Loma Prieta, California, earthquake: An anticipated event: Science, v. 247, p. 286–293.

Wallace, R.E., ed, 1990, The San Andreas fault system, California: United States Geological Survey Professional Paper 1515, 283 p.

Wei, W., and Johnson, A.M., in prep., Fault-folds—Handbook of Fold Form: Cambridge University Press.

Zhao, G., and Johnson, A.M., 1992, Sequence of deformations recorded in joints and faults, Arches National Park, Utah: Journal of Structural Geology, v. 14, no. 2, p. 225-236.

Appendix I. Details of Horizontal Surveys

This appendix explains the survey data that are presented in Appendix II and used in the computer program (Appendix III) to compute strains in the Granada Hills area. The data were compiled from the notebooks of surveyors employed by the City of Los Angeles. This appendix also contains a description of the types of permanent survey monuments, and notes on procedures.

We decided to work with strain rather than displacments. One could calculate coordinates for points and then displacement fields. However, error accumulates in such a procedure, and it is difficult to interpret the results, because a fixed point is determined arbitrarily. Furthermore, most damage to the ground and to structures results from differential displacement (strain), not absolute displacement. Thus our calculations are of length and angle changes. The strain calculations are necessarily estimates because an unknown amount of the differential displacement can result from displacements across discontinuities rather than of uniform deformation. The angle changes and the normalized length changes represent components of strain only if the deformation is homogeneous at the scale of the measurements.

Surveying Procedures

All distances and angles were measured using a total station survey system. The total station was set up over the benchmark using an optical plummet. Targets were also set over benchmarks on tripods using optical plummets. On many streets, in addition to the benchmarks at intersections, there were several added points surveyed along the centerline of a street. These points could be used to help relocate a lost point at an intersection by extrapolating the added points to the center of the intersection. This extrapolation along several streets would locate the position of the point in the intersection. If the lines from opposite streets did not match, the difference would be split to relocate the point. When measuring deviations from a line along the center of the street, the instrument would be aligned and pointed at the benchmark on the ground. The instrument operator then determined the offset by taking a reading directly off a steel tape placed on the ground.

The angle measurement procedure with the instrument at point A, and reflectors on points B and C, would be as follows:

The small angle between B and C could be measured in the face 1 and face 2 positions. The angle would then be corrected. The lower base of the total station would then be turned about 120°. The large angle between B and C would then be measured in the face 1 and face 2 positions, and this angle would be corrected. The large and small angle would then be summed, and the difference taken from 360°. The angles would then be adjusted by the same amount so that they summed to 360°. If any of the corrections required numbers greater than a few seconds, the angle measurements would be repeated. The turning of the lower base of the Total Station ensures that angles are measured on a different part of the horizontal circle, helping to distribute error.

Use of Data

The survey data are used to compare distances between the same material points at some time before and some time after the 1994 earthquake. This is perhaps the most accurate way to work with survey data. By using field measurements of distances between specific monuments, we restrict the

errors to those inherent in obtaining those particular measurements. Thus, an error in survey data will be restricted to a single intersection or single street segment, and will not propagate through a network of measurements. In contrast, there will be additional errors in angle measurements because they are corrected by closing around a block or a larger area, and the error is distributed, generally according to the lengths of the survey legs.

Accuracy of Survey Data in Relation to Strain Determinations

The City of Los Angeles regards their determination of distances to be accurate to one hundredth of a foot (0.01 ft) or 3.1 mm. For a street length of 100 m, the normalized error would be 3×10^{-5}. This can be verified by comparing results of different surveys done in the same areas provided there are no earthquakes between surveys. In interpreting the strain patterns from this study we have assumed that normalized length changes must be at least three times this large, at least 10^{-4}, to be significant. Thus, we assume that the error is on the order of 5 mm over a 50 m long block and 20 mm over a 200 m long block, with a change in angle of 0.27 seconds. Assuming that any error is distributed over both sets of measurements, the lengths would have to be incorrect by 2.5 to 10 mm, and angles by 16 seconds, in order to produce a "strain" of the size that we would regard as significant.

We can get an idea about the worst case error in distance measurement by looking at the instrument specifications. The electronic distance meter on the total station (Topcon GTS–3B) used for the measurements is accurate to 5mm ± 3 mm/km. The total station used in the surveys was taken out to a surveyed baseline and calibrated before use in Granada Hills. Over a small block, about 50 m in length, the error in distance measurement could be as large as 5 mm ± 3 x 0.05 mm, or 5.15 mm. Over a longer block distance, say 200 m, the error in distance measurement could be 5 ± 3 x 0.2 mm, or about 5.6 mm. Thus, the relative errors in length determination are of the order of 5×10^{-4} for the long block and 6×10^{-5} for the short block. In principal, then, strains of 10^{-4} to 10^{-5} can be determined.

We would note that, strains in the order of 10^{-4}, or smaller on blocks as short as 50 m, may represent error in the measurements. Strains of 10^{-3} on short blocks will represent deformation. For longer blocks, strains of 10^{-4} and larger will represent deformation. The blocks for which the data are questionable at the 10^{-4} level are the east–west streets connecting the north–south alleys on either side of Balboa Avenue. None of the strains in this area is as small as 10^{-4}; they are on the order of 10^{-3} or larger. Thus, even on the short blocks, the deformation is large enough to make us confident of the survey results.

According to the Los Angeles surveyors, angle measurements should have an error of less than 2 seconds; the total station used can measure angles to 3 seconds. The repeated measurement of an angle, however, and the use of double centering will improve the accuracy of the angles, (e.g., Moffitt and Bouchard, 1992). For an analysis of error, we will assume an error of 3 seconds. The shear strain is the tangent of the angle, so an angular error of 3 seconds corresponds to an apparent shear strain of 1.45×10^{-5}. Thus, angle measurements have an error that is comparable, if not less than, distance measurements, and shear strains can again be determined to about 10^{-5}. Again, since we are comparing two measurements which may contain this error, the real error is twice the magnitude of a single measurement.

We use 10^{-4} as a cutoff for strain determinations, so the strains are about an order of magnitude larger than the instrument error.

Monument Types

A source of error that we cannot quantify is the miss location of points. Since most survey points are centered over a tack or a punch hole, these errors will be less than 1 mm, and will not be systematic. Such errors are smaller than the errors of the distance meter in the total station, and thus cannot be detected. There are, however, different types of targets used for the surveys.

This study used both surface and subsurface, centerline monuments for the City of Los Angeles, located at the centerlines of roads and the centers of intersections. Subsurface monuments are buried beneath the roadfill prism. They normally consist of a concrete pillar encasing a steel pipe, with a cap on the pipe. The monument is accessed through a small cover. A second type of subsurface monument is the sewer-access vault, which extends below the roadfill material to the sewer level. These monuments consist of four hooks on the inside walls of the vault which, when joined by string, define the survey point. The vault can be inspected for signs of cracking or deformation during the survey.

Surface monuments are normally spikes or nails driven into the pavement. The nail may also be driven through a washer[1] or a circle of tin[2]. Other surface markers are lead–filled holes, with small tacks pounded into the lead[3], and old railroad spikes, which have been marked with a hole punch to define the survey marks.

Relocation of Points

Both surface and subsurface monuments are backed–up by a series of "tie–outs" or "throw–overs." Tie–outs are surface monuments that are a known distance and direction away from the center–line monument. There are usually at least four tie–outs. At some large intersections the tie–outs for subsurface monuments may be other subsurface monuments. Lost centerline monuments can be relocated using the tie–outs, or by determining the intersection of the centerlines of joining streets. Generally, tie–outs are used to determine the area where a careful search should be made for the original monument. Often an old monument was obscured by street work, such as patching. Within the study area, some of the intersections near Balboa Avenue were re–located using tie–outs, or matching centerlines of adjacent streets. This could put the data from these intersections (Intersections 17, 19, 20, 26, 29, 50) in doubt. Relocation of these points is probably within 0.1 feet (3 cm). For the intersections along Balboa Avenue, the changes in street length are going to be much larger than the error in re–locating a point. The sense of strain (extension or shortening) will not change, but the magnitude of the strain may be in error. It should be noted that, along Balboa Avenue, the total change in length between centerline monuments was the same as that measured using lot survey marks along the sidewalk.

[1] S & W for shorthand.
[2] S & T for shorthand.
[3] L & T for shorthand.

Measurement stations in the Balboa Area

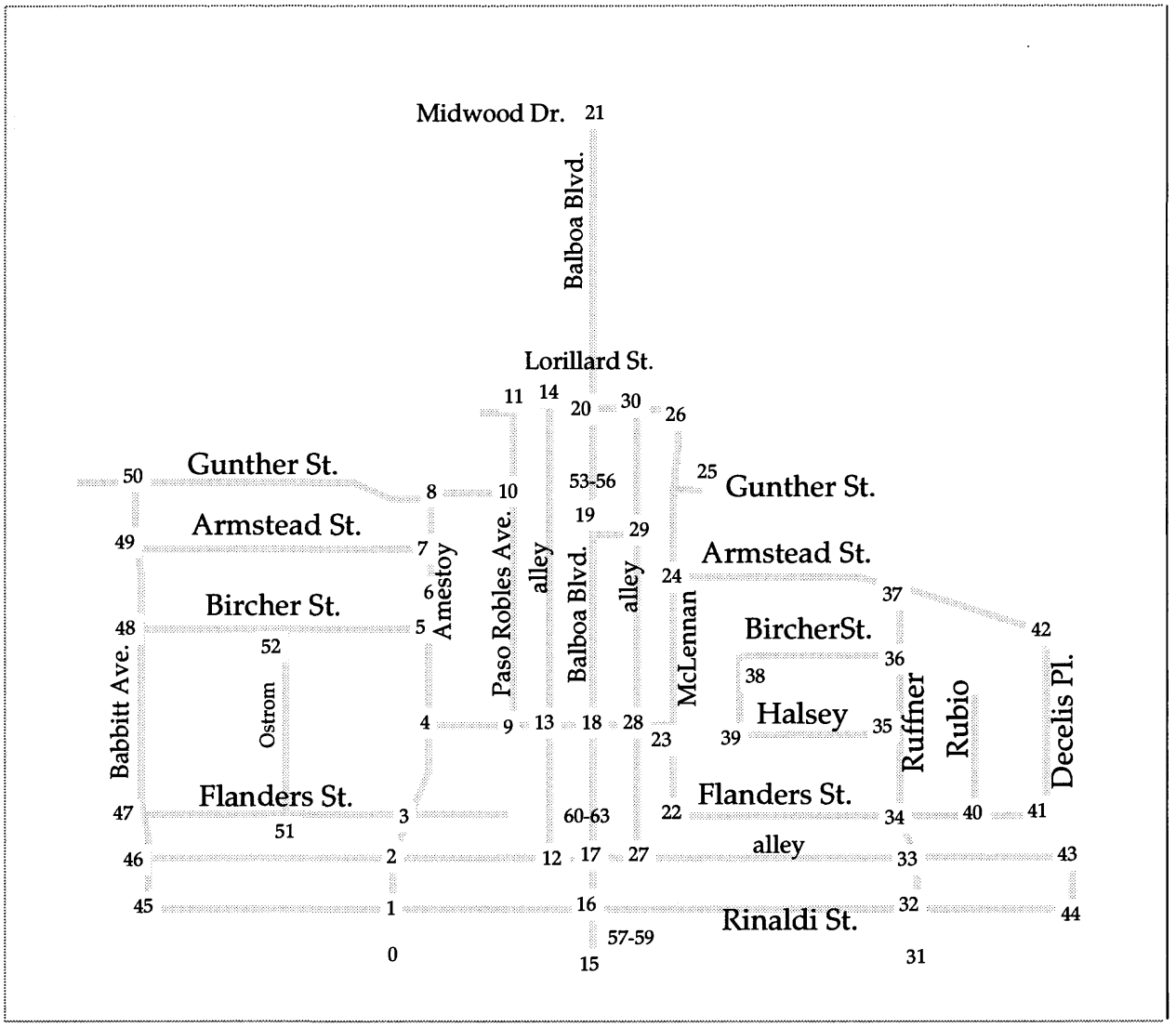

Figure 15. Locations and identification numbers of measurement stations in the Granada Hills area. Location numbers are used in Appendix II.

Appendix II. The Survey Data

Worksheet Columns and Abbreviations

This appendix contains the data used in this study. The data were compiled from a map produced by the City of Los Angeles and the Surveyor's field notebooks. The data included are:

Intersection Number. This corresponds to the numbering scheme used in this report. Intersection. Street names for the intersection (Figure 15).

Type. Type of Monument (SS: Sub–surface, S&T: Spike and tin, L&T: Lead and tack, S&W: spike and washer).

Field Books. City of Los Angeles field book numbers of the intersection. These field books contain all the data about monuments at that intersection.

The remainder of the columns contain the data used in the calculations. The parameters are defined in the text.

Explanation of Table of Survey Data

Feature	Abbreviation in Field Book
Surface Monument Type	
Spike and Tin	S&T
Spike and Washer	S&W
Lead and Tack	L&T
Spike	Spk
Chiseled X	Chx
Subsurface Monument Type	
Standard Survey Disc Monument	SSDM
Standard Survey Monument	SSM
Sewer Manhole Monument	SMHM
(Lead and Tack in manhole chimney.)	

Land Survey Data

No.	Intersection	Type	Field book pages	Quadrant	Alpha degree	Year	street lengths a	b	θ degr	min	sec	Notes
0	Amestoy and Alley	S&W	213–133–135	NE		1972	825.220	180.000	90	0	4	S. of Rinaldi
			213–135–213			1994	825.160	180.070	90	1	13	S&W found as tied out.
1	Rinaldi and Amestoy	S&W	213–133–135	NE	0	1964	825.210	180.000	90	0	0	S&W found as tied out.
						1972	825.240	180.170	90	0	4	
						1983	825.240	180.170	90	0	49	
						1994	825.180	180.130	90	0	49	
				NW	0	1964	993.640	180.000	90	0	0	
						1972	993.690	180.170	90	0	21	
						1983	993.700	180.170	90	0	21	
						1994	993.660	180.130	90	0	38	
				SE	0	1964	825.210	180.000	89	59	34	
						1972	825.240	180.000	89	59	56	
						1994	825.180	180.130	89	58	35	
2	S Alley/Amstoy	Spike	213–133–140	NE	0	1972	645.370	160.840	67	–48	–21	
						1994	645.280	160.860	67	–47	26	
				SW	0	1964	993.640	180.000	89	59	19	
						1983	993.690	180.170	89	59	19	
						1994	993.680	180.130	89	59	9	
				SE	0	1964	645.250	180.000	89	59	56	
						1972	645.370	180.170	89	59	35	
						1983	645.280	180.170	89	59	35	
						1994	645.280	180.130	89	59	21	
3	Flanders/Amstoy	SS	213–133–144	NE		1972	420.930	185.640	65	12	0	SMHM set in 1983. SMHM found in 1994.
						1994	420.960	185.730	65	13	56	
4	Halsey/Amstoy	SS	213–133–164	NE	0	1964	348.260	330.610	90	0	34	SMHM found in 1994.
						1972	348.670	330.710	90	0	33	
						1983	348.670	330.710	90	0	33	
						1994	349.050	330.780	90	13	6	
5	Bircher and Amestoy	Spike	213–133–166	NW	0	1964	579.700	143.000	90	0	43	Spike found in 1994.
						1972	579.720	143.050	90	1	6	
						1983	579.720	143.050	90	1	6	
						1994	579.730	143.180	89	59	11	
6	Amestoy/Tract Line	Spike	213–133–202	NW		1972	10.000	137.000	90	0	53	Spike and L&T found 1994.
						1994	10.000	136.920	89	36	37	
				SE		1972	10.000	143.050	90	0	53	S&W set by tract lines & distance in 1994.
						1994	10.000	143.180	89	35	55	

7	Armstead and Amestoy	Spike	213–133–203	NW		1972	1172.840	66.380	90	0	43	Found N-S spikes in 1994. Reset S&W using ties.
						1994	1173.190	66.400	89	59	52	
8	Gunther/Amstoy	S&T	213–133–170	SW	0	1964	41.780	140.000	89	58	37	
				SE	0	1964	338.200	140.000	90	0	0	
						1972	338.560	140.080	89	57	54	
						1983	338.560	140.000	89	57	54	
						1994	338.620	140.030	89	56	12	
9	Halsey/Paso Robles	SS	213–133–163	NE	0	1972	151.370	816.960	90	1	26	SSDM found in 1994. S&W set in 1994.
						1994	151.490	818.100	90	9	31	
				NW	0	1964	348.260	817.050	89	59	26	
						1972	348.670	816.960	89	58	34	
						1983	348.670	816.960	89	58	34	
						1994	349.050	818.100	89	45	6	
10	Gunther/Paso Robles	SS	213–133–169	NW		1972	338.560	280.010	89	56	21	SSDM found in 1994.
						1994	338.620	280.130	89	54	27	
				SW	0	1964	338.200	817.050	90	0	0	
						1983	338.560	816.960	90	3	39	
						1994	338.620	818.100	90	6	35	
11	Lorillard/Paso Robles	S&W	213–133–172	NW	0	1964	172.000	276.550	90	0	0	S&W found in 1994.
						1983	172.000	276.480	90	0	0	
				SE	0	1964	151.360	280.000	90	0	0	
						1972	151.370	280.010	90	0	0	
						1983	151.370	280.010	90	0	0	
						1994	151.400	280.130	89	59	32	
12	W Alley/S Alley	L&T	213–133–139	NE	0	1972	179.960	466.260	90	0	20	L&T found 1994. S&W set in 1994.
						1994	180.070	464.900	89	57	55	
				NW	0	1964	645.250	466.200	90	0	0	
						1972	645.370	466.260	89	59	40	
						1983	645.370	466.260	89	59	40	
						1994	645.280	464.900	90	3	32	
13	Halsey/W Alley	Spike S&W	213–133–162	NE	0	1964	180.000	1120.520	90	0	3	Spike found in 1994. S&W set by intersection.
						1972	179.970	1120.490	90	0	3	
						1983	179.970	1120.490	90	5	45	
						1994	179.970	1122.030	90	5	45	
				NW	0	1964	151.360	1120.520	89	59	26	
						1972	151.370	1120.490	89	58	39	
						1983	151.370	1120.490	89	58	39	
						1994	151.490	1122.030	89	50	29	
				SW	0	1964	151.360	466.200	90	0	34	
						1972	151.370	466.260	90	0	34	
						1983	151.370	166.260	90	3	36	
						1994	151.490	464.900	90	3	36	
				SE	0	1964	180.000	466.200	89	59	26	
						1972	179.970	466.260	89	59	26	
						1983	179.970	166.260	90	0	10	
						1994	179.970	464.900	90	0	10	

14	Lorillard/W Alley	S&W	213–133–171	NW	0	1964	151.360	1152.830	90	0	0	S&W found
						1983	151.370	1152.860	90	0	1	in 1994.
				SW		1972	151.370	1120.490	90	0	0	
						1994	151.400	1122.030	90	1	30	
				SE		1972	10.000	1120.490	90	0	0	
						1994	10.000	1122.030	90	–1	–30	
15	Alley S of Rinaldi and Balboa	S&T	213–133–125	NW		1972	1.000	180.060	90	0	0	S&T found in
						1994	1.000	180.080	90	0	13	1994.
16	Balboa and Rinaldi	S&W	213–133–174	NE		1972	1320.360	177.030	90	0	0	S&W found in
						1994	1320.390	177.150	89	55	40	1994.
				NW		1972	823.240	177.030	90	0	43	
						1994	823.180	177.150	90	2	36	
				SW	0	1972	823.240	180.000	90	0	1	
						1994	823.180	180.080	90	0	59	
				SE		1972	1320.360	180.000	89	59	16	
						1994	1320.390	180.080	90	0	45	
17	S Alley/Balboa	S&W	213–133–138	NE	0	1964	180.000	463.180	89	59	43	S&W set by ties
						1972	180.000	463.260	90	0	0	in 1994.
						1994	179.780	461.860	89	55	34	
				NW	0	1964	180.000	463.180	90	0	43	
						1972	179.960	463.260	90	0	43	
						1983	179.960	463.260	89	59	44	
						1994	180.070	461.860	90	1	19	
18	Halsey/Balboa	S&T	213–133–161	NE	0	1964	180.000	666.940	90	0	34	S&T found in
						1972	180.025	666.940	90	0	0	1994. New S&T
						1983	180.025	666.940	90	0	0	set by ties in
						1994	180.100	667.320	90	5	5	1994.
				NW	0	1972	179.970	666.940	89	59	26	
						1994	179.970	667.320	89	54	15	
				SW	0	1964	180.000	463.180	90	0	34	
						1972	179.970	463.260	90	1	21	
						1983	179.970	463.260	90	1	21	
						1994	179.970	461.860	90	0	36	
				SE	0	1972	180.025	463.260	90	0	4	
						1994	180.100	461.860	89	58	39	
19	Balboa/N Alley	S&W	213–133–111	NE		1972	180.000	435.050	90	0	0	Set S&W in
						1994	180.010	436.360	89	59	17	1994.
				SE		1964	180.000	667.000	90	0	9	
						1972	180.000	666.940	90	0	0	
						1994	180.010	667.320	91	–59	–17	
20	Lorillard and Balboa	S&W	213–133–110	NE		1972	180.000	347.310	90	0	0	S&T found in
						1994	179.950	347.325	90	2	–12	1994.
				NW	–5	1964	170.640	347.332	84	59	12	
						1972	170.640	347.310	84	57	60	
						1994	170.640	347.325	360	0	0	
				SW	–5	1972	170.640	435.050	95	2	0	
						1994	170.640	436.360	95	5	6	
				SE	0	1972	180.000	435.050	90	0	0	
						1994	179.950	436.360	89	57	33	

21	Balboa and Midwood Drive	L&T	213–133–106	SW	0	1964	1.000	772.148	90	0	20	L&T found in 1994.
						1972	1.000	772.060	90	0	0	
						1994	1.000	772.020	90	0	0	
22	Flanders/McLennan	SS	213–133–119	NE	0	1964	927.060	317.100	89	59	31	SSDM set in 1973. SSDM found in 1994.
						1972	927.140	317.190	90	0	50	
						1994	927.160	315.940	89	51	56	
23	Halsey/McLennan	SS	213–133–118	NW	0	1964	146.000	520.100	89	59	26	SSDM found in 1994.
						1972	145.985	519.970	90	4	6	
						1994	146.070	520.740	90	3	32	
				SW	0	1964	146.000	317.100	90	0	24	
						1972	145.985	317.190	89	55	54	
						1994	146.070	315.940	89	47	38	
24	Armstead/McLennan	SS	213–133–117	NE	0	1964	776.820	277.420	90	0	29	SSDM found in 1994.
						1994	776.440	277.740	89	57	30	
				SE	0	1964	776.820	520.100	89	59	31	SSDM found in 1994.
						1972	776.905	519.970	89	59	31	
						1994	776.440	520.740	90	2	10	
25	Gunther/McLennan	SS	PE–2G–821	NE	0	1972	122.390	182.840	84	49	35	SMHM found in 1994.
			213–133–190			1994	122.390	183.010	84	53	5	
				SE		1972	122.390	27.870	96	–49	–35	New SSDM set in 1994 .
						1994	122.390	28.190	96	–53	–5	
26	McLennan N. of Lorillard	S&W	213–133–193	NE		1972	1.000	210.390	90	0	0	S&W set by ties in 1994.
						1994	1.000	210.440	90	0	0	
				SW		1972	165.000	94.700	90	0	0	
						1994	165.080	94.700	90	1	38	
27	S Alley/E Alley	X	213–133–113	NW	0	1964	180.000	463.140	90	0	17	Chiseled 'X' found in 1994.
			213-133-195			1994	179.780	461.640	90	6	48	
28	Halsey/E Alley	S&T	213–133–114	NE	0	1964	146.000	667.050	89	55	16	S&T found in 1994.
						1994	146.070	667.625	89	56	36	
				NW	0	1964	180.000	667.050	89	59	26	
						1994	180.100	667.625	89	54	27	
				SW	0	1964	180.000	463.140	90	1	14	
						1994	180.100	461.640	89	57	34	
				SE	0	1964	146.000	463.140	90	5	21	
						1994	146.070	461.640	90	11	23	
29	N Alley/E Alley	Spike	213–133–115	NW	0	1972	180.000	435.010	91	–59	–30	Spike & L&T set in 1994.
						1994	180.010	436.195	91	–59	–45	
				SW	0	1964	180.000	667.050	89	59	41	
						1994	180.010	667.652	89	59	45	
30	E Alley/Lorillard	S&W	213–133–198	SW		1972	180.000	435.010	90	0	0	S&W found 1994 as tied out.
						1994	179.950	436.195	91	–57	–5	
				SE		1972	165.000	435.010	90	0	0	
						1994	165.080	436.195	89	57	5	

32	Rinaldi and Ruffner	SS	213–137–108	NE	0	1964	640.320	160.000	90	0	0	SSDM found
						1972	640.599	160.055	89	54	45	in 1994.
						1994	640.620	160.130	89	54	50	
				NW	0	1964	1320.360	160.000	90	0	0	
						1972	1320.390	160.055	90	5	11	
						1994	1320.390	160.130	90	5	11	
33	S Alley/Ruffner	S&T	213–137–120	NW	0	1964	1132.240	179.110	67	56	27	S&T found
						1972	1132.530	179.200	67	55	30	in 1994 as
						1994	1132.530	179.050	67	57	30	tied out.
				SW	0	1964	1132.240	160.000	90	0	0	
						1972	1132.530	160.055	90	–6	20	
						1994	1132.530	160.130	90	–3	–17	
34	Ruffner and Flanders	SS	213–137–119	NE	0	1964	289.000	283.000	90	0	0	SSDM & Brass
						1972	288.950	283.005	90	0	55	disk found
						1994	288.820	282.990	89	57	50	in 1994.
				NW	0	1964	927.060	283.000	89	59	5	
						1972	927.140	283.005	90	3	18	
						1994	927.160	282.990	90	3	18	
				SW	0	1964	927.060	179.110	112	4	25	
						1972	927.140	179.200	112	0	12	
						1994	927.160	179.050	112	2	13	
				SE	0	1964	289.000	179.110	67	56	27	
						1972	288.950	179.200	67	55	35	
						1994	288.820	179.050	67	56	39	
35	Ruffner/Halsey	SS	213–137–118	NW	0	1964	651.490	274.000	90	0	0	SMHM found
						1972	651.240	274.070	90	7	48	in 1994.
						1994	651.240	274.070	90	7	48	
				SW	0	1964	651.490	283.000	90	0	0	
						1972	651.240	283.005	89	49	46	
						1994	651.240	282.990	89	49	46	
36	Ruffner/Bircher	SS	213–137–117	NW	0	1964	651.490	160.830	90	0	0	SMHM found
						1972	651.490	160.775	89	57	52	in 1994.
						1994	651.490	160.890	89	57	52	
				SW	0	1964	651.490	274.000	90	0	0	
						1972	651.490	274.040	90	0	0	
						1994	651.490	274.070	89	57	58	
37	Armstead and Ruffner	SS	213–137–115	SW	–9	1964	176.230	75.790	90	0	0	SMHM found
						1972	176.250	75.745	90	4	24	in 1994.
						1994	176.240	75.770	90	4	24	
				SE	2	1964	575.240	75.790	90	0	0	
						1972	575.490	75.745	89	58	—	
						1994	575.480	75.770	89	54	45	
38	Bircher/Bircher	Bolt & T	213–133–120	SE	0	1964	651.490	274.000	90	0	0	Bolt & T found
						1994	651.490	275.160	89	58	54	in 1994. S&W
												set in 1994
												by intersection.
39	Bircher/Halsey	S&T	213–133–121	NE	0	1964	651.490	274.000	90	0	2	S&T found
						1994	651.240	275.160	89	55	20	in 1994.

40	Flanders and Rubio	S&T	213–137–126	NW	0	1964	289.000	420.000	90	0	0	S&T found
						1972	288.950	420.270	90	0	9	in 1994.
						1994	288.820	420.270	90	1	24	
41	Decelis and Flanders	S&T	213–137–122	NW	0	1964	286.000	640.020	90	0	0	S&T found
						1972	286.055	640.020	89	59	54	in 1994.
						1994	286.070	640.060	90	1	31	
42	Armstead and Decelis	SS	213–133–121	SW	–8	1964	575.240	640.020	105	12	41	SMHM found
						1972	575.490	640.020	105	12	30	in 1994.
						1994	575.480	640.060	105	11	45	
43	E.E. Alley and S. Alley	L&T	213–137–124	SW	0	1964	648.450	180.000	89	59	27	L&T found
						1994	648.510	180.100	89	59	27	in 1994.
44	Rinaldi and E.E. Alley	SS	213–137–125	NW	0	1964	640.320	180.000	89	59	28	SSDM found
						1972	640.599	180.100	89	59	27	in 1994.
						1994	640.620	180.100	90	0	42	
45	Babbitt and Rinaldi	S&W	213–133–136	NE	0	1964	993.640	180.000	90	0	0	"S&W found
						1972	993.690	180.060	90	0	0	in 1994, not as
						1983	993.700	180.060	89	59	51	tied out".
						1994	993.660	180.070	89	59	51	
				NW	0	1964	822.000	180.000	90	0	0	
						1983	821.840	180.060	90	0	19	
				SW	0	1964	822.000	140.260	90	0	0	
46	S. Alley and Babbitt	S&W	213–133–141	NE		1983	993.690	83.800	90	0	43	S&W found
						1994	993.680	83.800	90	0	43	in 1994.
				SE	0	1964	993.640	180.000	90	0	0	
						1972	993.690	180.060	90	0	39	
						1983	993.690	180.060	90	9	39	
						1994	993.680	180.070	90	0	21	
47	Flanders and Babbitt	Spike	213–133–150	NE	0	1964	281.180	62.640	97	10	9	Spike found
						1972	281.180	62.600	97	10	9	in 1994 as
						1983	281.180	62.600	97	10	9	tied out.
						1994	281.180	62.580	97	10	11	
				NW	0	1964	311.190	62.640	82	49	53	
						1983	311.040	62.600	82	49	51	
48	Bircher and Babbitt	SS	213–133–168	SE	0	1964	575.000	588.850	90	0	0	SMHM found
						1972	575.250	589.140	89	59	12	in 1994.
						1983	575.250	589.140	89	59	12	
						1994	575.270	589.220	89	58	50	
49	Armstead and Babbit	S&T	PE–3D–92	NE	0	1964	1172.840	80.690	95	37	2	S&T found
			213–133–206			1972	1172.840	80.690	95	37	2	as tied out.
						1994	1173.190	80.640	95	37	5	
50	Gunther and Babbit	SS	PE–3D–89	SE	0	1964	277.000	194.700	89	59	46	SMHM set in
			213–133–208			1972	277.000	194.700	89	59	46	1994 by
						1994	277.020	194.700	89	58	23	intersection.

52	Bircher and Ostrom	SS	213–133–167	SE	0	1964	579.760	651.000	90	0	0	SMHM found
						1972	579.720	651.160	90	0	12	in 1994.
						1983	579.720	651.160	90	0	12	
						1994	579.730	651.250	90	0	4	
53	Near Lorillard and Balboa (Note dummy data 1.0 in all of following)			NE		1972	1.000	162.000	90	0	0	
						1994	1.000	162.070	90	0	0	
54	Balboa #2			NE		1972	1.000	81.000	90	0	0	
						1994	1.000	81.060	90	0	0	
55	Balboa #3			NE		1972	1.000	81.020	90	0	0	
						1994	1.000	81.150	90	0	0	
56	Balboa #4			NE		1972	1.000	10.000	90	0	0	
						1994	1.000	11.030	90	0	0	
57	Balboa near Rinaldi			NE		1972	1.000	177.050	90	0	0	
						1994	1.000	177.150	90	0	0	
58	Balboa near alley near Rinaldi			NE		1972	1.000	60.000	90	0	0	
						1994	1.000	60.050	90	0	0	
59	Just N. of 58			NE		1972	1.000	60.000	90	0	0	
						1994	1.000	60.130	90	0	0	
60	Compression stretch			NE		1972	1.000	60.000	90	0	0	
						1994	1.000	58.660	90	0	0	
61	Balboa between Halsey and alley			NE		1972	1.000	60.000	90	0	0	
						1994	1.000	60.140	90	0	0	
62	Near Halsey on Balboa			NE		1972	1.000	60.000	90	0	0	
						1994	1.000	60.060	90	0	0	
63	Balboa near Halsey (note dummy data 1.0)			NE		1972	1.000	114.140	90	0	0	
						1994	1.000	113.840	90	0	0	

Appendix III. NERDSMOO.BAS©—Listing of QuickBasic Computer Program Used to Analyze Strains

QUICKBASIC© program NERDSMOO©
for entering survey data computing strains
and preparing an AUTOCAD© file for a drafting program.
by
A.M. Johnson
PURDUE UNIVERSITY
June 1996

```
REM  Saved as <NERDSMOO.bas>
   CLS
   nMax = 100: PRINT
   hold$ = "r"
   'x and z are coordinates of intersection,AA,a are lengths in x–direction
   ' BB, b are lengths in other street direction, xoffset and zoffset determine
   ' where shmoo is to be plotted. Atheta(i) is orientation of street a relative to east
   ' counterclockwise angles positive.
   ' Four sets of data, 1, 2 3,4  for three times.
   DIM x(nMax), z(nMax)
   DIM year$(4), Quad$(4)
   DIM a(4, 4, nMax), b(4, 4, nMax)
   DIM xoffset(4, nMax), zoffset(4, nMax), Alpha(4, nMax)
   DIM name$(nMax), index%(nMax)
   DIM Atheta(4, 3, 4, nMax), Btheta(4, 3, 4, nMax)
   DIM E1(4, nMax), E2(4, nMax), BBtheta(kk, nMax)
   DIM dxdX(4, nMax), dxdZ(4, nMax), dzdX(4, nMax), dzdZ(4, nMax)
         CLS
         Quad$(1) = "NE": Quad$(2) = "NW": Quad$(3) = "SW": Quad$(4) = "SE"
         pi = 4 * ATN(1)
         co = pi / 180
         format1$ = "#####.##"
         format2$ = "########"
         GOSUB first.part:
n = 0
PRINT "To proceed, you need to select an option:"
   PRINT "If there is no file, do <1>. Else, do another option"
   PRINT
   PRINT
options:
   PRINT "Type <1> to ENTER Intersection,length and angle DATA from keyboard."
   ' Note that <1> STARTS a NEW file.
   PRINT "Type <2> to ADD Intersection, length and angle DATA from keyboard."
   PRINT "Type <3> to ADD Length and Angle Data from keyboard."
   PRINT "Type <4> to CHANGE some Length or Angle Data."
   PRINT "Type <5> to READ and EXAMINE a data file."
   PRINT "Type <6> to FILL IN a data file or LPRINT a data file."
   PRINT "Type <7> to READ a *.dat file, PROCESS the data, CREATE a *.pro file"
   PRINT " and CREATE a *.dxf file for an autocad map."
   PRINT "Type <8> to READ a *.pro file and CREATE a *.dxf file for an autocad map."
   PRINT "Type <9> to READ a *.pro file, CHANGE RESULTS, and CREATE a *.dxf file for an autocad map."
   PRINT "Type <10> to READ and EXAMINE a *.pro file."
   PRINT "Type <11> to READ a *.dat file and MAKE a document file."
```

```
INPUT "Which is it, <1 OR 2 OR 3 OR 4 OR 5 or 6 or 7 or 8 or 9 or 10 or 11> —>"; ans
   IF ans > 11 OR ans < 1 THEN GOTO options:


'**********************START THE OPTIONS*********************
IF ans <> 1 THEN GOTO skip1:
'     ENTER Intersection,length and angle DATA from keyboard.
          GOSUB enter.intersection.data:
skip1:
'*********
IF ans <> 2 THEN GOTO skip2:
'     ADD Intersection, length and angle DATA from keyboard.
          GOSUB file:
          GOSUB add.intersections:
          GOSUB save:
skip2:
'*********
IF ans <> 3 THEN GOTO skip3:
'     ADD Length and Angle Data from keyboard.
          GOSUB file:
          GOSUB add.lengths.angles:
          GOSUB save:
skip3:
'********
IF ans <> 4 THEN GOTO skip4:
'     CHANGE some Length or Angle Data
          GOSUB file:
          GOSUB change.results:
          GOSUB save:
skip4:
'********
IF ans <> 5 THEN GOTO skip5:
'     READ and EXAMINE a data file.
          GOSUB file:
          GOSUB examine.data:
skip5:
'********
IF ans <> 6 THEN GOTO skip6:
'     READ and a data file fill in missing data and then LPRINT it.
          GOSUB file:
          GOSUB fill.in.data.set:
          INPUT "Do you wish to Lprint data file (type <y> or <n>)"; ans$
          IF ans$ = "y" OR ans$ = "yes" THEN GOSUB lprint.the.data:
skip6:
'*******
IF ans <> 7 THEN GOTO skip7:
'     READ a *.dat file, PROCESS the data, CREATE a *.pro file
'     and CREATE a *.dxf file for an autocad map.
          CLS
          GOSUB file:
          GOSUB create.pro:
          GOSUB make.autocad.file:
skip7:
' ******
IF ans <> 8 THEN GOTO skip8:
```

```
'     READ a *.pro file and CREATE a *.dxf file for an autocad map.
          GOSUB read.profile:
          GOSUB make.autocad.file:
skip8:
'*******
IF ans <> 9 THEN GOTO skip9:
'     READ a *.pro file, CHANGE RESULTS, and CREATE a *.dxf file for an autocad map.
          GOSUB read.profile:
          GOSUB make.changes:
          GOSUB save.profile:
          GOSUB make.autocad.file:
skip9:
' *******
IF ans <> 10 THEN GOTO skip10:
'     READ and EXAMINE a *.pro file.
          GOSUB read.profile:
          CLS
          GOSUB examine.pro:
skip10:
IF ans <> 11 THEN GOTO skip11:
'     READ a *.dat file and MAKE a document file.
          GOSUB file:
          GOSUB print.the.data.to.a.file:
skip11:
' *****Send a carriage return and end program.
LPRINT CHR$(27) + CHR$(69)     ' this ejects paper.
END
' **********************END OF MAIN PROGRAM *************************
' ****************************************************************
'**********************BEGIN SUBROUTINES ***************************
' ****************************************************************
REM *******************save:************************
' save *.dat file.
save:
   PRINT
   PRINT "FILE IS BEING SAVED TO HARD DISK"
   filein$ = filename$
          m = INSTR(filein$, ".")
          IF m <> 0 THEN filein$ = LEFT$(filein$, m - 1)
          filein$ = filein$ + ".dat"
   CLS
   OPEN filein$ FOR OUTPUT AS #2
          FOR j = 1 TO 4       ' j is no of year
                    WRITE #2, year$(j)
          NEXT
          FOR i = 0 TO nn
           ' i is number of street intersection
                    WRITE #2, name$(i), x(i), z(i)
                    FOR kk = 1 TO 4
                              WRITE #2, xoffset(kk, i), zoffset(kk, i), Alpha(kk, i)
                              ' j is the year
                              FOR j = 1 TO 4
                                        WRITE #2, a(j, kk, i), b(j, kk, i)
                                        FOR k = 1 TO 3   ' k is degr, min or sec
                                                  WRITE #2, Btheta(j, k, kk, i)
```

```
                                NEXT
                            NEXT
                        NEXT
            NEXT
    CLOSE #2
RETURN

'********************enter name of files*************************
name.of.file:
    PRINT "Enter only first part of name. <.dat> or <.dat> will be added automatically"
    PRINT "Name must be 7 or fewer letters and numbers"
    INPUT "Data are in file with name"; filename$
RETURN

' **********************file****************************
' Open the data file.
file:
    PRINT
    GOSUB name.of.file:
    filein$ = filename$
            m = INSTR(filein$, ".")
            IF m <> 0 THEN filein$ = LEFT$(filein$, m - 1)
            filein$ = filein$ + ".dat"
    CLS
    OPEN filein$ FOR INPUT AS #2
            FOR j = 1 TO 4        ' j is no of year
                    INPUT #2, year$(j)
            NEXT
ii = 0
DO UNTIL EOF(2)
             ' ii is number of street intersection
                    INPUT #2, name$(ii), x(ii), z(ii)
                    FOR kk = 1 TO 4
                            INPUT #2, xoffset(kk, ii), zoffset(kk, ii), Alpha(kk, ii)
                            ' j is the year
                            FOR j = 1 TO 4
                                    INPUT #2, a(j, kk, ii), b(j, kk, ii)
                                    FOR k = 1 TO 3   ' k is degr, min or sec
                                            INPUT #2, Btheta(j, k, kk, ii)
                                    NEXT
                            NEXT
                    NEXT
ii = ii + 1
LOOP
CLOSE #2
nn = ii - 1
RETURN
' *************************create.pro**********************
create.pro:
REM READ a *.dat file, PROCESS the data and create a *.pro file.
enter1:
            REM ****select the two years****
    INPUT "Which data set will be initial state <1, 2,3 or 4>"; j1
    INPUT "Which data set will be final state"; j2
    PRINT "Initial state will be"; year$(j1), "and final state will be"; year$(j2)
```

```
   INPUT "Do you wish to select an optional year in case year 1 is blank <y,n Enter is n>?"; answer$
   j3 = j1
   IF answer$ = "y" THEN
         INPUT "optional year <1,2 or 3>"; j3
   END IF
   IF j3 = 0 OR j3 > 3 THEN
         PRINT "Must be between 1 and 3; try again, idiot!"
         GOTO enter1:
   END IF
   INPUT "Are these O.K. <if yes, just enter; if no, type n>"; answer$
   IF answer$ = "n" THEN GOTO enter1:
   GOSUB determine.extension.components:
   GOSUB save.profile:
RETURN
' *************************read.pro file ***********************
read.profile:
'  read file with .pro extension (extensions)
  IF filename$ = "" THEN GOSUB name.of.file:
  filein$ = filename$
         m = INSTR(filein$, ".")
         IF m <> 0 THEN filein$ = LEFT$(filein$, m - 1)
         filein$ = filein$ + ".pro"
   CLS
   OPEN filein$ FOR INPUT AS #2
         i = 1
         INPUT #2, year1$, year2$, j1

         DO UNTIL EOF(2)
          ' i is number of street corner
                INPUT #2, name$(i), x(i), z(i)
           FOR kk = 1 TO 4
                INPUT #2, xoffset(kk, i), zoffset(kk, i), Alpha(kk, i)
                INPUT #2, E1(kk, i), E2(kk, i), dxdX(kk, i), dxdZ(kk, i), dzdX(kk, i), dzdZ(kk, i)
           NEXT
         i = i + 1
         LOOP
   CLOSE #2
   ' set maximum number of data to i-1
   nn = i - 1
RETURN
' ****************************save.profile.******************
save.profile:
REM   save file of processed extension data
   fileout$ = filename$
   CLS
         m = INSTR(fileout$, ".")
         IF m <> 0 THEN fileout$ = LEFT$(fileout$, m - 1)
         fileout$ = fileout$ + ".pro"
   OPEN fileout$ FOR OUTPUT AS #2
         WRITE #2, year$(j1), year$(j2), j1
         FOR i = 0 TO nn
          ' i is number of street corner
                WRITE #2, name$(i), x(i), z(i)
           FOR kk = 1 TO 4
                WRITE #2, xoffset(kk, i), zoffset(kk, i), Alpha(kk, i)
```

```
                WRITE #2, E1(kk, i), E2(kk, i), dxdX(kk, i), dxdZ(kk, i), dzdX(kk, i), dzdZ(kk, i)
            NEXT
        NEXT
    CLOSE #2
RETURN
REM ************************Determine.extension.Components**************************
determine.extension.components:
j0 = j1
FOR i = 0 TO nn
        CLS
        j1 = j0
  FOR kk = 1 TO 4
    IF ABS(Btheta(j1, 1, kk, i) * Btheta(j2, 1, kk, i)) < 1 THEN
        IF ABS(Btheta(j3, 1, kk, i) * Btheta(j2, 1, kk, i)) < 1 THEN GOTO skip50:
        j1 = j3
    END IF
    IF a(j2, kk, i) * a(j1, kk, i) < 1 THEN GOTO skip50:
    IF b(j2, kk, i) * b(j1, kk, i) < 1 THEN GOTO skip50:
    Sa = a(j2, kk, i) / a(j1, kk, i)
    Sb = b(j2, kk, i) / b(j1, kk, i)
    IF Sa = 1 AND Sb = 1 THEN GOTO skip50:
    Ea = Sa - 1
    Eb = Sb - 1
    Bthet = 0
    Bcapthet = 0
        FOR k = 1 TO 3
            Bthet = Bthet + Btheta(j2, k, kk, i) / (60 ^ (k - 1))
            Bcapthet = Bcapthet + Btheta(j1, k, kk, i) / (60 ^ (k - 1))
        NEXT
        jump$ = "yes"
        IF ABS(Bthet) < 89 OR ABS(Bthet) > 91 THEN jump$ = "no"
REM ****assign the sign according to the quadrant
        IF kk = 2 OR kk = 4 THEN index% = 2
        IF kk = 1 OR kk = 3 THEN index% = 1
        Bcapthet = 180 * (index% - 1) - Bcapthet * (-1) ^ index%
        Bthet = 180 * (index% - 1) - Bthet * (-1) ^ index%

    Bt = Bthet + Alpha(kk, i)
    Bct = Bcapthet + Alpha(kk, i)
    'IF Alpha(kk, i) < 0 THEN Alpha(kk, i) = Alpha(kk, i) + 360
    IF Bct < 0 THEN Bct = Bcapthet + Alpha(kk, i) + 360
    IF Bt < 0 THEN Bt = Bthet + Alpha(kk, i) + 360
        PRINT "We are working on intersection"; name$(i)
        dxdZ(kk, i) = (Sb * COS(Bthet * co) - Sa * COS(Bcapthet * co)) / SIN(Bcapthet * co)
        dxdX(kk, i) = Sa
        dzdX(kk, i) = 0
        dzdZ(kk, i) = Sb * SIN(Bthet * co) / SIN(Bcapthet * co)
adjust.deform.gradients:
        CLS 2
        PRINT "dxdX="; dxdX(kk, i), "dxdZ="; dxdZ(kk, i), "dzdZ="; dzdZ(kk, i)
    ' scale the window
    zscale = 5 * (ABS(1 - dxdX(kk, i)) + ABS(dxdZ(kk, i)) + ABS(1 - dzdZ(kk, i))) / 3
SCREEN 2
    VIEW (20, 2)-(620, 172), , 1
```

```
    WINDOW (0, –1)–(360, 1)
    CLS 2
    ' print two known stretches
    LINE (Bt – 4, Eb / zscale + .04)–(Bt + 4, Eb / zscale – .04), , B
    LINE (Bct – 4, Eb / zscale + .04)–(Bct + 4, Eb / zscale – .04), , B
    LINE (Bt + 180 – 4, Eb / zscale + .04)–(Bt + 180 + 4, Eb / zscale – .04), , B
    LINE (Bct + 180 – 4, Eb / zscale + .04)–(Bct + 180 + 4, Eb / zscale – .04), , B
    LINE (Alpha(kk, i) – 4, Ea / zscale + .04)–(Alpha(kk, i) + 4, Ea / zscale – .04), , B

    ' print the curves

    REM Fit data to extension distribution
    FOR thet = 0 TO 360 STEP 5
        D = (dxdX(kk, i) * dzdZ(kk, i) – dxdZ(kk, i) * dzdX(kk, i))
        temp1 = (dzdZ(kk, i) * COS(thet * co) – dxdZ(kk, i) * SIN(thet * co)) ^ 2
        temp2 = (–dzdX(kk, i) * COS(thet * co) + dxdX(kk, i) * SIN(thet * co)) ^ 2
        E1st = (–1 + D / SQR(temp1 + temp2)) / zscale
        IF thet > 0 THEN
            LINE (thet0 + Alpha(kk, i), t1)–(thet + Alpha(kk, i), E1st)
            ' LINE (thet0 + Alpha(kk, i), t2)–(thet + Alpha(kk, i), E2nd)
        END IF
        thet0 = thet
        t1 = E1st
    NEXT
    i1 = (dxdX(kk, i) ^ 2) + (dzdZ(kk, i) ^ 2) + (dxdZ(kk, i) ^ 2) + (dzdX(kk, i) ^ 2)
    i2 = D ^ 2
        test = (i1 ^ 2) – 4 * i2
   IF test < 0 THEN
        test = 0
        PRINT "Warning—Negative square root!!!"
    END IF
    S1 = SQR((1 / 2) * (i1 + SQR(test)))
    S2 = SQR((1 / 2) * (i1 – SQR(test)))
        E1(kk, i) = S1 – 1
        E2(kk, i) = S2 – 1
    ' There is no check if streets are at right angles
        IF jump$ = "yes" THEN GOTO skip23:

        VIEW PRINT 1 TO 5

        PRINT name$(i), "E1"; E1(kk, i), "E2"; E2(kk, i)
        PRINT "Just Checking. Points should lie on line. Push a key to continue"
    DO: LOOP WHILE INKEY$ = ""      ' wait for a key press

    CLS 2   '  clear text viewport
skip23:
CLS 1
CLS 2
    IF print$ = "yes" THEN
        LPRINT
        LPRINT
        LPRINT "extension data for intersection"; i
        LPRINT name$(i), "quadrant", Quad$(kk)
        LPRINT "coordinates", x(i), z(i)
        LPRINT "offsets", xoffset(kk, i), zoffset(kk, i)
```

```
        LPRINT "lengths", a(j1, kk, i), a(j2, kk, i), b(j1, kk, i), b(j2, kk, i)
        LPRINT "deformation gradient dxdX, dxdZ, dzdX, dzdZ"
        LPRINT dxdX(kk, i), dxdZ(kk, i), dzdX(kk, i), dzdZ(kk, i)
        LPRINT "principal extensions E1, E2"; E1(kk, i), E2(kk, i)
        LPRINT "The deformation gradient dxdX is in the direction "; n; ";90–Alpha(kk,i);"; E; ""
        LPRINT "and dzdZ is at right angles."
        LPRINT : LPRINT : LPRINT
        END IF
skip50:
  NEXT
NEXT
IF print$ = "yes" THEN LPRINT CHR$(27) + CHR$(69)
RETURN
REM**************************calculation of extensions complete*********

REM *********************************make.autocad.file*****************

make.autocad.file:
        CLS
        INPUT "Do you want to create a file for plotting of map? <y OR n> –> ", answer$
        IF answer$ = "n" THEN END
        PRINT "Please be patient. This takes a little time."
        PRINT "I will ask you to push a key when I am finished."
        PRINT "Thank you, oh patient master!"
        PRINT " The extension analysis is based on the following notions:"
        PRINT " (1) The extension is exactly described in terms of four components"
        PRINT " of the deformation gradient, dx/dX, dx/dZ, dz/dX, dz/dZ."
        PRINT " The stretches are measured along two directions, a and b."
        PRINT " The original angle (cap theta) between a and b and the final"
        PRINT " angle (theta) are known. Theta positive if counterclockwise from"
        PRINT " a–axis. Rotation is of no interest, we we can assume dz/dX = 0."
        PRINT " The axis a is the reference direction, before and after deformation."
        PRINT " The change in orientation of b relative to a is determined by simple"
        PRINT " shear parallel to a. This determines dx/dZ. The stretch in a is dx/dX."
        PRINT " The stretch in b is adjusted until the measurements define a possible"
        PRINT " state of extension. In general, the component dz/dZ is closely related to"
        PRINT " the stretch in b; is should be equal if the final angle between a and b"
        PRINT " is 90 degrees. Finally, the results are checked by plotting extension as a"
        PRINT " as a function of lower–and upper–case thetas."

        section$ = "SECTION"
        polyline$ = "POLYLINE"
        entities$ = "ENTITIES"
        vertex$ = "VERTEX"
        seqend$ = "SEQEND"
        endsec$ = "ENDSEC"
        eof$ = "EOF"
        fileout$ = filename$
        m = INSTR(fileout$, ".")
        IF m <> 0 THEN fileout$ = LEFT$(fileout$, m – 1)
        filout1$ = fileout$ + "1.dxf"
        filout2$ = fileout$ + "2.dxf"
        filout3$ = fileout$ + "3.dxf"
        xfact = 5
        blank$ = CHR$(0)
```

```
OPEN filout1$ FOR OUTPUT AS #3
        PRINT #3, 0
        PRINT #3, section$
        PRINT #3, 2
        PRINT #3, entities$
        PRINT #3, 0
OPEN filout2$ FOR OUTPUT AS #4
        PRINT #4, 0
        PRINT #4, section$
        PRINT #4, 2
        PRINT #4, entities$
        PRINT #4, 0

        rr = 5
        FOR i = 0 TO nn
           FOR kk = 1 TO 4
                temp1 = ABS(E1(kk, i))
                temp2 = ABS(E2(kk, i))
                refstr = temp1
                IF refstr < temp2 THEN refstr = temp2
                IF refstr = 0 THEN GOTO jump51:
                r = -(LOG(refstr) / LOG(10))
                IF r > rr THEN r = .99999 * rr' the smallest extension we can measure is 10-rr
                D = dxdX(kk, i) * dzdZ(kk, i) - dxdZ(kk, i) * dzdX(kk, i)
                PRINT #3, polyline$
                PRINT #3, 8
                PRINT #3, 0
                PRINT #3, 66
                PRINT #3, 1
                PRINT #3, 0
                radius = ((rr - r) ^ 2) / xfact
                FOR thet = 0 TO 360 STEP 5
                        th = (thet + Alpha(kk, i)) * co
                        tmp = ((dzdZ(kk, i) * COS(th) - dxdZ(kk, i) * SIN(th)) ^ 2) + ((-dzdX(kk, i) * COS(th) + dxdX(kk, i) *
SIN(th)) ^ 2)
                        str = (-1 + D / SQR(tmp)) / refstr
                        xx = xoffset(kk, i) + x(i) + radius * (1 + str) * COS(th)
                        zz = zoffset(kk, i) + z(i) + radius * (1 + str) * SIN(th)
                        PRINT #3, vertex$
                        PRINT #3, 8
                        PRINT #3, 0
                        PRINT #3, 10
                        PRINT #3, xx
                        PRINT #3, 20
                        PRINT #3, zz
                        PRINT #3, 0
                NEXT
                PRINT #3, seqend$
                PRINT #3, 8
                PRINT #3, 0
                PRINT #3, 0
                ' start a new image
                PRINT #4, polyline$
                PRINT #4, 8
                PRINT #4, 0
```

```
                PRINT #4, 66
                PRINT #4, 1
                PRINT #4, 0
                FOR thet = 0 TO 360 STEP 5
                        th = (thet + Alpha(kk, i)) * co
                        xxc = xoffset(kk, i) + x(i) + radius * COS(th)
                        zzc = zoffset(kk, i) + z(i) + radius * SIN(th)
                        PRINT #4, vertex$
                        PRINT #4, 8
                        PRINT #4, 0
                        PRINT #4, 10
                        PRINT #4, xxc
                        PRINT #4, 20
                        PRINT #4, zzc
                        PRINT #4, 0
                NEXT
                PRINT #4, seqend$
                PRINT #4, 8
                PRINT #4, 0
                PRINT #4, 0
jump51:
          NEXT
        NEXT

        ' The following routine provides data for scales of shmoos
                rmax = 1
        FOR ra = rmax TO rr STEP .5
                r = ra
                xx = -5
                zz = 45 + 4 * r
                ' start a new image
                PRINT #4, polyline$
                PRINT #4, 8
                PRINT #4, 0
                PRINT #4, 66
                PRINT #4, 1
                PRINT #4, 0
                FOR thet = 0 TO 360 STEP 5
                        th = thet * co
                        xxc = xx + (((rr - r) ^ 2) / xfact) * COS(th)
                        zzc = zz + (((rr - r) ^ 2) / xfact) * SIN(th)
                        PRINT #4, vertex$
                        PRINT #4, 8
                        PRINT #4, 0
                        PRINT #4, 10
                        PRINT #4, xxc
                        PRINT #4, 20
                        PRINT #4, zzc
                        PRINT #4, 0
                NEXT
                PRINT #4, seqend$
                PRINT #4, 8
                PRINT #4, 0
                PRINT #4, 0
        NEXT
```

```
        PRINT #4, seqend$
        PRINT #4, 8
        PRINT #4, 0
        PRINT #4, 0
        PRINT #4, endsec$
        PRINT #4, 0
        PRINT #4, eof$
        PRINT #4,
CLOSE #4
        PRINT #3, seqend$
        PRINT #3, 8
        PRINT #3, 0
        PRINT #3, 0
        PRINT #3, endsec$
        PRINT #3, 0
        PRINT #3, eof$
        PRINT #3,
CLOSE #3

                ' start lines for streets
OPEN filout3$ FOR OUTPUT AS #5
        PRINT #5, 0
        PRINT #5, section$
        PRINT #5, 2
        PRINT #5, entities$
        PRINT #5, 0
                CLS
read.next.line:
                PRINT #5, polyline$
                PRINT #5, 8
                PRINT #5, 0
                PRINT #5, 66
                PRINT #5, 1
                PRINT #5, 0
read.next.point:
                READ xxc, zzc
                IF xxc = 9999 THEN GOTO no.more.streets:
                IF xxc = 999 THEN GOTO end.of.line:
                        PRINT #5, vertex$
                        PRINT #5, 8
                        PRINT #5, 0
                        PRINT #5, 10
                        PRINT #5, xxc
                        PRINT #5, 20
                        PRINT #5, zzc
                        PRINT #5, 0
                        GOTO read.next.point:
end.of.line:
                PRINT #5, seqend$
                PRINT #5, 8
                PRINT #5, 0
                PRINT #5, 0
                GOTO read.next.line:
no.more.streets:
```

```
        PRINT #5, seqend$
        PRINT #5, 8
        PRINT #5, 0
        PRINT #5, 0
        PRINT #5, endsec$
        PRINT #5, 0
        PRINT #5, eof$
        PRINT #5,
CLOSE #5
RETURN

REM ************************fill.in.data.set************************
fill.in.data.set:
  IF hold$ = "h" THEN RETURN ' This will prevent data from being filled–in
  FOR iii = 0 TO nn
        FOR jj = 1 TO 4
                FOR k = 1 TO 4
                        kc = 5 – k
                        IF a(jj, k, iii) = 0 THEN a(jj, k, iii) = a(jj, kc, iii)
                        kp = 3 – k
                        IF k > 3 THEN kp = kp + 4
                        IF b(jj, k, iii) = 0 THEN b(jj, k, iii) = b(jj, kp, iii)
                NEXT
'complete the angles, if possible
        deg = 0: min = 0: sec = 0: ct = 0
    IF Btheta(jj, 1, 1, iii) * Btheta(jj, 1, 2, iii) * Btheta(jj, 1, 3, iii) <> 0 THEN ij = 4: ct = 1
    IF Btheta(jj, 1, 4, iii) * Btheta(jj, 1, 1, iii) * Btheta(jj, 1, 2, iii) <> 0 THEN ij = 3: ct = ct + 1
    IF Btheta(jj, 1, 3, iii) * Btheta(jj, 1, 4, iii) * Btheta(jj, 1, 1, iii) <> 0 THEN ij = 2: ct = ct + 1
    IF Btheta(jj, 1, 2, iii) * Btheta(jj, 1, 3, iii) * Btheta(jj, 1, 4, iii) <> 0 THEN ij = 1: ct = ct + 1
        IF ct <> 1 THEN GOTO skip52:
                FOR k = 1 TO 4
                        IF k <> ij THEN
                        deg = deg + Btheta(jj, 1, k, iii)
                        min = min + Btheta(jj, 2, k, iii)
                        sec = sec + Btheta(jj, 3, k, iii)
                        END IF
                NEXT
        mint = INT(sec / 60)
        IF Btheta(jj, 1, ij, iii) = 0 THEN
                Btheta(jj, 3, ij, iii) = 60 – (sec – mint * 60)
                min = min + mint
                degt = INT(min / 60)
                Btheta(jj, 2, ij, iii) = 59 – (min – degt * 60)
                Btheta(jj, 1, ij, iii) = 359 – deg + degt
    END IF
skip52:
        NEXT
NEXT
RETURN
'*****************************print.intersection*********************
print.intersection:
PRINT "Intersection number= "; i, "Location "; name$(i), "x= "; x(i), "z= "; z(i)
RETURN
' ********************print data**********************
print.data:
```

```
PRINT Quad$(kk); " corner(no."; kk; ")"; "xo= "; xoffset(kk, i), "zo= "; zoffset(kk, i); "  Alpha; Orientation of street a:"; Alpha(kk, i)
PRINT "              "; year$(1); "         "; year$(2); "          "; year$(3); "          "; year$(4)
PRINT "length a   :"; : PRINT USING format1$; a(1, kk, i); a(2, kk, i); a(3, kk, i); a(4, kk, i)
PRINT "length b   :"; : PRINT USING format1$; b(1, kk, i); b(2, kk, i); b(3, kk, i); b(4, kk, i)
PRINT "Angle Btheta:";
PRINT USING format2$; Btheta(1, 1, kk, i); Btheta(1, 2, kk, i); Btheta(1, 3, kk, i);
PRINT "_";
PRINT USING format2$; Btheta(2, 1, kk, i); Btheta(2, 2, kk, i); Btheta(2, 3, kk, i);
PRINT "_";
PRINT USING format2$; Btheta(3, 1, kk, i); Btheta(3, 2, kk, i); Btheta(3, 3, kk, i);
PRINT "_";
PRINT USING format2$; Btheta(4, 1, kk, i); Btheta(4, 2, kk, i); Btheta(4, 3, kk, i)
RETURN

REM ************************lengths.and.angles************************
lengths.and.angles:

        CLS
        GOSUB print.intersection:
        FOR kk = 1 TO 4
                GOSUB print.data:
        NEXT
change.quadrant:
    CLS
        PRINT : PRINT "To do a different intersection, or to quit, enter 0"
        INPUT "Which corner <kk> <1,2,3,4 or 0 to switch>"; kk
        IF kk = 0 THEN GOTO skip21:
        IF kk > 4 THEN GOTO change.quadrant:
    PRINT "Corner is"; Quad$(kk); " quadrant"
    PRINT : PRINT "The x–offset of the shmoo (in cm!)": INPUT " –>"; xoffset(kk, i)
    PRINT "The z–offset of the shmoo (in cm!)": INPUT " –>"; zoffset(kk, i)
    INPUT "Orientation of street a is (degrees)"; Alpha(kk, ii)
        CLS
please:
        PRINT "Now enter information on year, lengths and angles"
        PRINT "To do a different intersection, or to quit, enter 0"
        INPUT "Which year <1,2 3,4 or 0 to switch>"; j
        IF j = 0 THEN GOTO change.quadrant:
        IF j > 4 THEN
                PRINT "Enter correct year for data set, dumbo!"
                GOTO please:
        END IF
        PRINT "Data for year"; year$(j)
        INPUT "Is this the correct year< n or y Enter is y>"; answer$
  IF answer$ = "n" THEN
        PRINT "Enter correct quadrant and year for data set, you cretin!"
        GOTO please:
  END IF
        CLS
        PRINT "intersection"; i, name$(i)
        PRINT "Quadrant"; Quad$(kk), "Lengths and Angle:"
        PRINT "a and b and Btheta"; a(j, kk, i); b(j, kk, i), Btheta(j, 1, kk, i); Btheta(j, 2, kk, i); Btheta(j, 3, kk, i)
        INPUT "Change lengths or angle <n, y or q; Enter is y>"; answer$
        IF answer$ = "n" OR answer$ = "q" THEN GOTO skip21:
        GOSUB enter.lengths:
```

```
        GOTO please:
skip21:
GOSUB save:
RETURN
REM ************************enter.lengths*****************************
enter.lengths:
        CLS
        PRINT "intersection"; i, name$(i), "Quadrant"; Quad$(kk)
        PRINT "year is "; year$(j), "   Lengths and Angle:"
        PRINT "length a="; a(j, kk, i)
        INPUT "Is this length O.K. <y,n Enter is y>"; answer$
        IF answer$ = "n" THEN
          PRINT "What is length of street a (runs ca E–W)": INPUT a(j, kk, i)
        END IF
        PRINT "length b="; b(j, kk, i)
        INPUT "Is this length O.K. <y,n Enter is y>"; answer$
        IF answer$ = "n" THEN
          PRINT "What is length of street b (runs ca N_W)": INPUT b(j, kk, i)
        END IF
        PRINT "The lengths of strees a and b are"; a(j, kk, i), b(j, kk, i)
        PRINT "Now enter angles angles as degrees, minutes and seconds"
                PRINT "Note! Measure angles counterclockwise from east!"
                PRINT
                PRINT "The orientation of street a is"; Alpha(kk, i)
        INPUT "If this is O.K. then push Enter, Else type n"; answer$
        IF answer$ <> "" THEN
                PRINT : PRINT "The orientation of street a": INPUT "degrees –>"; Alpha(kk, i)
        END IF

        PRINT : PRINT "The angle between streets a and b in"; Quad$(kk), " quadrant is";
                PRINT Btheta(j, 1, kk, i); Btheta(j, 2, kk, i); Btheta(j, 3, kk, i)
                PRINT "To hold this angle at 0, enter 360"
                INPUT "If this is O.K. then push Enter, Else type n"; answer$
                IF answer$ <> "" THEN
                        PRINT "The angle between streets a and b is"
                        INPUT "degrees –>"; Btheta(j, 1, kk, i)
                        INPUT "minutes –>"; Btheta(j, 2, kk, i)
                        INPUT "seconds–>"; Btheta(j, 3, kk, i)
                END IF

    ko = kk
    FOR kk = 1 TO 4
                GOSUB print.data:
    NEXT
    kk = ko
    PRINT : INPUT "IS THE INFORMATION ENTERED ABOVE CORRECT? <y OR n Enter is y> –> "; answer$
    IF answer$ = "n" THEN GOTO enter.lengths:
RETURN
REM ********************change.results************************
change.results:
    hold$ = "h"
    CLS
    FOR j = 1 TO 4
        PRINT : PRINT "year of"; j; "th data set", year$(j)
        INPUT "correct <y or n Enter is y>"; answer$
```

```
        IF answer$ = "n" THEN INPUT "year"; year$(j)
    NEXT
which.one:
        CLS
        PRINT "Enter 0 to end changes and EXIT."
        INPUT "Which intersection <1....39....70 etc.or 0>"; i
        IF i = 0 THEN GOTO skip22:
        IF i > nn THEN GOTO which.one:
        GOSUB correct.intersection:
another.corner:
        CLS
        GOSUB print.intersection:
        FOR kk = 1 TO 4
                GOSUB print.data:
        NEXT
        PRINT : PRINT "intersection is no."; i, name$(i)
        PRINT "Answer 0 (zero) to do another intersection or exit"
        INPUT "Which corner <1,2,3,4 or 0>"; kk
        IF kk = 0 THEN GOTO which.one:
        IF kk > 4 THEN GOTO another.corner:
        PRINT "Corner is "; Quad$(kk)
another.year:
        PRINT "Answer 0 (zero) to do another corner or intersection or exit"
        INPUT "Which year <1,2,3,4 or 0>"; j
        IF j = 0 THEN GOTO which.one:
        IF j > 4 THEN GOTO another.year:
        GOSUB enter.lengths:

        PRINT "year is "; year$(j)
        INPUT "Another year <y or n Enter is y>—>"; answer$
        IF answer$ <> "n" THEN GOTO another.year:
        INPUT "Another corner <y or n Enter is y>"; answer$
        IF answer$ <> "n" THEN GOTO another.corner:
        INPUT "Another intersection <y or n Enter is y>"; answer$
        IF answer$ <> "n" THEN GOTO which.one:
skip22:
GOSUB save:
RETURN

REM ******************enter.intersection*************************
enter.intersection:

    end$ = "n"
    PRINT "To stop entry of data, push <enter> when asked for name of intersection."
type.in.data:
    PRINT "The previous intersection is:"; name$(i – 1)
    PRINT : PRINT i; "(Name) The intersection of street1/street2": INPUT " –>"; name$(i)
    IF name$(i) = "" THEN nn = i – 1: end$ = "y": RETURN
    PRINT "The x–coordinate of the intersection": INPUT " –>"; x(i)
    PRINT "The z–coordinate of the intersection": INPUT " –>"; z(i)
    PRINT "datum set"; i; "intersection"; name$(i)
    PRINT : INPUT "IS THE INFORMATION ENTERED ABOVE CORRECT? <y OR n> –> "; answer$
    IF answer$ = "n" THEN
        GOSUB correct.intersection:
    END IF
```

```
RETURN
REM ************************correct.intersection*****************
correct.intersection:
    CLS
    PRINT "Note that you can answer yes by simply pushing <Enter>"
    PRINT "but that you must answer no by typing n"
    PRINT : PRINT i; "Intersection of "; name$(i)
    INPUT "Is this name correct <y or n Enter is y>"; answer$
    IF answer$ <> "n" THEN GOTO try.again:
    INPUT "intersection"; name$(i)
    GOTO correct.intersection:
try.again:
    INPUT "Quadrant no. NE=1; NW=2; SW=3; SE=4"; kk
    IF kk = 0 OR kk > 4 THEN GOTO try.again:
    PRINT : PRINT "Quadrant is"; Quad$(kk)
    INPUT "Is this quadrant correct <y or n Enter is y>"; answer$
    IF answer$ = "n" THEN INPUT "Quadrant number is"; kk
positions:
    PRINT "x– and z–positions of the intersection are"; x(i), z(i)
    INPUT "Are these positions correct <y or n Enter is y>"; answer$
    IF answer$ = "n" THEN
        INPUT "x–position ofintersection is"; x(i)
        INPUT "z–position ofintersection is"; z(i)
    END IF
offsets:
    PRINT "i="; i, "intersection="; name$(i)
    PRINT : PRINT "X– and Z–offsets of the shmoo (in cm!) are"; xoffset(kk, i), zoffset(kk, i)
    INPUT "Are these offsets correct <y or n Enter is y>"; answer$
    IF answer$ = "n" THEN
        INPUT "X–offset of the shmoo (in cm!) is"; xoffset(kk, i)
        INPUT "Z–offset of the shmoo (in cm!) is"; zoffset(kk, i)
    END IF
RETURN
REM ****************************make.changes*******************************
make.changes:
CLS
PRINT "Note that you can answer yes by simply pushing <Enter>"
    PRINT "but that you must answer no by typing n"
    PRINT : PRINT i; "Intersection of "; name$(i)
    INPUT "Is this name correct <y or n>"; answer$
    IF answer$ = "n" THEN INPUT "intersection"; name$(i)
    IF name$(i) = "" THEN n = n – 1: PRINT "A null data set": RETURN
PRINT "x– and z–positions of the intersection are"; x(i), z(i)
    INPUT "Are these positions correct <y or n>"; answer$
    IF answer$ = "n" THEN
        INPUT "x–position ofintersection is"; x(i)
        INPUT "z–position ofintersection is"; z(i)
    END IF
PRINT "i="; i, "intersection="; name$(i)
FOR kk = 1 TO 4
    PRINT : PRINT "x– and z–offsets of the shmoo (in cm!) are"; xoffset(kk, i), zoffset(kk, i)
    INPUT "Are these offsets correct <y or n>"; answer$
    IF answer$ = "n" THEN
        INPUT "X–offset of the shmoo (in cm!) is"; xoffset(kk, i)
        INPUT "Z–offset of the shmoo (in cm!) is"; zoffset(kk, i)
```

```
    END IF
NEXT
   CLS
RETURN
' ************************examine.pro**********************
examine.pro:
        PRINT "As you read the data sets, push <q> to quit or any other key"
        PRINT "to read the next data set. Run option ???3 "
        PRINT "to modify data sets and save data set."
        PRINT
        PRINT "Push any key to continue"

        DO WHILE INKEY$ = "": LOOP
        j = j2
        PRINT "year", year$(j)
        FOR i = 1 TO n
          ' i is number of street corner

                CLS
                PRINT "intersection "; i, name$(i)
                PRINT "x-coord "; x(i), "z-coord "; z(i)
                FOR kk = 1 TO 4
                        PRINT "x-offset "; xoffset(kk, i)
                        PRINT "z-offset "; zoffset(kk, i)
                        PRINT "principal extensions "; E1(kk, i), E2(kk, i)
                        PRINT "Components of displacement gradient"
                        PRINT "dxdX(kk,i), dxdZ(kk,i), dzdX(kk,i), dzdZ(kk,i)"
                        PRINT dxdX(kk, i), dxdZ(kk, i), dzdX(kk, i), dzdZ(kk, i)
                        PRINT "Orientation of street a "; Alpha(kk, i)
                        PRINT "Angle between streets a and b "; Btheta(j, 1, kk, i); Btheta(j, 2, kk, i); Btheta(j, 3, kk, i)
                        tp$ = ""
                        DO WHILE tp$ = ""
                        tp$ = INKEY$
                        IF tp$ = "q" THEN GOTO skip7:
                        LOOP
                NEXT
        NEXT
RETURN
' **********************enter.intersection.data*********************
enter.intersection.data:
  i = 1
  CLS
  DO
        PRINT "Starting a new data set (number=)"; i
        GOSUB enter.intersection:
        GOSUB save:
        i = i + 1
        nn = nn + 1
  LOOP UNTIL end$ = "y"
RETURN
'*****************************add.intersections*****************
add.intersections:
        i = nn + 1
        CLS
        DO
```

```
                PRINT "Starting a new data set (number=)"; i
                GOSUB enter.intersection:
                IF end$ = "y" THEN GOTO skip24:
                GOSUB lengths.and.angles:
                GOSUB save:
                i = i + 1
                nn = nn + 1
skip24:
        LOOP UNTIL end$ = "y"
RETURN
add.lengths.angles:
do.another:
        CLS
        PRINT "To quit, type in <q> when asked a question"
        INPUT "Make a(nother) change <n, y or q Enter is y>"; answer$
        IF answer$ = "q" OR answer$ = "n" THEN GOTO skip13:

try.a.different.one:
        INPUT "Number of intersection"; i
        IF i > nn THEN
                PRINT "there are only "; nn; " intersections "; ""
                GOTO try.a.different.one
        END IF
        PRINT "intersection"; i, name$(i)
        INPUT "Is this the one you wanted <n or y; Enter is y>"; answer$
        IF answer$ = "n" THEN GOTO try.a.different.one:
        GOSUB lengths.and.angles:
        GOSUB save:
        GOTO do.another:
skip13:
RETURN
' ************************examine.data************************
examine.data:
        CLS
        PRINT "As you read the data sets, push <q> to quit or any other key"
        PRINT "to read the next data set."
        PRINT
        PRINT "Push any key to continue"

        DO WHILE INKEY$ = "": LOOP

        FOR i = 0 TO nn
                '  m = 0
                ' this section strips the prefix
                ' m = INSTR(Name$(i), "NE ")
                ' IF m = 0 THEN m = INSTR(Name$(i), "NW ")
                ' IF m = 0 THEN m = INSTR(Name$(i), "SW ")
                ' IF m = 0 THEN m = INSTR(Name$(i), "SE ")
                ' IF m <> 0 THEN MID$(Name$(i), m, 3) = "   "
                CLS
                PRINT "push <q> to quit"
                FOR kk = 1 TO 4
                        GOSUB print.intersection:
                        GOSUB print.data
                        INPUT "push enter"; tp0
```

```
                NEXT
                CLS
                PRINT "push a key <or q to quit>"
                tp$ = ""
                DO WHILE tp$ = ""
                tp$ = INKEY$
                IF tp$ = "q" THEN GOTO skip15:
                LOOP
        NEXT
skip15:
RETURN
' ******************print.the.data.to.a.file***************************************
print.the.data.to.a.file:
        fileout$ = filename$
        m = INSTR(fileout$, ".")
        IF m <> 0 THEN fileout$ = LEFT$(fileout$, m - 1)
        fileout$ = fileout$ + ".doc"
        OPEN fileout$ FOR OUTPUT AS #3
        WRITE #3, TITLE$
                xst$ = "It is "
                xst1$ = "hours on "
        WRITE #3, xst$, TIME$, xst1$, DATE$
                xstb$ = "Intersection number = "
                xst$ = "Corner "
                xst1$ = "Atheta; Orientation of street a:"
                xst2$ = "x-offset ="
                xst3$ = "z-offset ="
                xst4$ = "year    :"
                xst5$ = "length a   :"
                xst6$ = "length b   :"
                xst7$ = "Angle Btheta:"
                xstc$ = "Location"
                xst1c$ = "x-coord (feet) = "
                xstd$ = "z-coord (feet) = "
FOR i = 0 TO nn
        WRITE #3, xstb$, i
        WRITE #3, xstc$, name$(i)

                WRITE #3, xst1c$, x(i), xstd$, z(i)
        FOR kk = 1 TO 4
                WRITE #3, xst$, Quad$(kk)
                WRITE #3, xst2$, xoffset(kk, i), xst3$, zoffset(kk, i)
                WRITE #3, xst1$, Alpha(kk, i)
                WRITE #3, xst4$
                WRITE #3, year$(1), year$(2), year$(3), year$(4)
                WRITE #3, xst5$
                WRITE #3, a(1, kk, i), a(2, kk, i), a(3, kk, i), a(4, kk, i)
                WRITE #3, xst6$
                WRITE #3, b(1, kk, i), b(2, kk, i), b(3, kk, i), b(4, kk, i)
                WRITE #3, xst7$
                WRITE #3, Btheta(1, 1, kk, i), Btheta(2, 1, kk, i), Btheta(3, 1, kk, i), Btheta(4, 1, kk, i)
                WRITE #3, Btheta(1, 2, kk, i), Btheta(2, 2, kk, i), Btheta(3, 2, kk, i), Btheta(4, 2, kk, i)
                WRITE #3, Btheta(1, 3, kk, i), Btheta(2, 3, kk, i), Btheta(3, 3, kk, i), Btheta(4, 3, kk, i)
        NEXT
NEXT
```

```
CLOSE #3
RETURN
REM **********firstpart**********
first.part:
  PRINT "-------------------------------------------------------------"
  PRINT " Analysis of Changes of Street Length and Angle Between Streets"
  PRINT "in one-quarter of an intersection. NERDSMOO, VERSION 1.6 (1996)"
  PRINT " extension Analysis, version 1.5, based on an excel program."
  PRINT " Written in 1995 by A.M. Johnson."
  PRINT "-------------------------------------------------------------"
  PRINT
  PRINT "It is "; TIME$; " hours  on "; DATE$
  PRINT
  INPUT "Enter descriptive title of run  --> "; TITLE$
  CLS
  PRINT "A *.dat file is a file produced by this program. It contains information about"
  PRINT "intersections, lengths & angles. An existing *.dat file can be manipulated by this program."
  PRINT "A *.pro file is a processed *.dat file that contains extension information."
  PRINT "This program can manipulate an existing *.pro file."
  PRINT "A *.dxf file is a processed *.pro file. It is an AUTOCAD file that DESIGNER can read"
' It can, that is, if you have changed the  mgx.ini  file to include the two lines:

' [Translation]
' EnableAltTrans=1

  PRINT "The *.dxf file contains details of shmoos and nerds and the streets."
  PRINT "Note that information on streets is entered via data statements at end of program."
  PRINT : PRINT
RETURN

' **********lprint.the.data**********
lprint.the.data:
IF print$ <> "y" THEN RETURN
FOR i = 0 TO nn
CLS
        LPRINT : LPRINT "Intersection number= "; i, "Location "; name$(i)
                LPRINT "x-coord "; x(i), "z-coord "; z(i)
        FOR kk = 1 TO 4
                LPRINT : LPRINT Quad$(kk); " corner"
                LPRINT "x-offset "; xoffset(kk, i), "z-offset "; zoffset(kk, i)
                LPRINT "Atheta; Orientation of street a:"; Alpha(kk, i)
                LPRINT "year      :"
                LPRINT "              "; year$(1); "      "; year$(2); "      "; year$(3); "      "; year$(4)
                LPRINT "length a   :"; : LPRINT USING format1$; a(1, kk, i); a(2, kk, i); a(3, kk, i); a(4, kk, i)
                LPRINT "length b   :"; : LPRINT USING format1$; b(1, kk, i); b(2, kk, i); b(3, kk, i); b(4, kk, i)

                LPRINT "Angle Btheta:"; : LPRINT USING format2$; Btheta(1, 1, kk, i); Btheta(2, 1, kk, i); Btheta(3, 1, kk, i); Btheta(4,
1, kk, i)
                LPRINT "          "; : LPRINT USING format2$; Btheta(1, 2, kk, i); Btheta(2, 2, kk, i); Btheta(3, 2, kk, i); Btheta(4, 2,
kk, i)
                LPRINT "          "; : LPRINT USING format2$; Btheta(1, 3, kk, i); Btheta(2, 3, kk, i); Btheta(3, 3, kk, i); Btheta(4, 3,
kk, i)
        NEXT
NEXT
LPRINT CHR$(27) + CHR$(69)
```

```
RETURN

'————————————END————————————————
' _————————————data on streets at Balboa————————

' the pair of numers 999,999 signifies end of polyline
DATA –25.1,0,20.8,0,54.1,0,54.1,4,52.3,8.2,52.3,26.5,52.8,28.4,48.3,29.5
DATA 29,29.6,29,36.6,29.6,42.1,29.6,44.5,20.8,44.6,16.25,44.9,12.5,44.9
DATA 12.5,37.05,3.95,37.05,3.95,28.25,3.75,28.25,3.75,16.15,3.75,12.25
DATA 0,4.5,0,0,999,999
DATA 20.8,0,20.8,60,999,999
DATA –25.1,4.5,54,4.5,999,999
DATA 67.5,8.25,29,8.25,29,29.6,999,999
DATA 52.3,15.5,35.8,15.5,35.8,22.6,52.3,22.6,999,999
DATA –25.5,8.4,11.9,8.4,999,999
DATA 3.75,16.4,29.1,16.4,999,999
DATA 21,33.4,25.5,33.4, 999,999
DATA 29,37.4,32,37.4,999,999
DATA 3.5,24.9,–26,24.9,999,999
DATA 3.8,32.1,–26,32.1,999,999
DATA 12.3,44.2,9,44.2, 999,999
DATA 12.45,16.4,12.45,37.2,999,999
DATA 16.25,4.6,16.25,45,999,999
DATA 25.3,4.6,25.3,44.6,999,999
DATA 54.1,0,70.26095,0,70.26095,4.54112,53.90096,4.54112,999,999
DATA 70.26095,0,70.74026,0
DATA 60,8.5,60,19.09536,999,999
DATA 67.5,8.5,67.5,24.64682,53.01968,28.5,999,999
DATA 20.8,44,20.8,72,999,999
DATA 20.8,0,20.8,–4.5,999,999
DATA 3.5,36.5,0,36.5,–4,38,–26.5,38,999,999
DATA 0,0,–25.1,0,–25.1,6.2,–25.9,9.8,–25.9,29.9,–26.5,33.9,–26.5,38.5,999,999
DATA –11,8.4,–11,24.9,999,999
DATA 60,65,51,65,51,42,60,42,999,999
DATA 59,41,51,41,51,40
' The pair of numbers 9999,9999 defines the end of the data set
DATA 9999,9999

' ————————————END————————————
```